BCL2-ASSOCIATED ATHANOGENE4 Regulates the KAT1 Potassium Channel and Controls Stomatal Movement[1][OPEN]

Antonella Locascio,[a] Maria Carmen Marqués,[a] Guillermo García-Martínez,[a] Claire Corratgé-Faillie,[b] Nuria Andrés-Colás,[a] Lourdes Rubio,[c] José Antonio Fernández,[c] Anne-Aliénor Véry,[b] José Miguel Mulet,[a] and Lynne Yenush[a,2,3]

[a]Instituto de Biología Molecular y Celular de Plantas, Universitat Politécnica de Valencia-Consejo Superior de Investigaciones Científicas, 46022 Valencia, Spain

[b]Biochimie et Physiologie Moléculaire des Plantes, Université Montpellier, Centre National de la Recherche Scientifique, Institut National de la Recherche Agronomique (INRA), SupAgro Montpellier, Campus SupAgro-INRA, 34060 Montpellier Cedex 2, France

[c]Facultad de Ciencias, Universidad de Málaga, Campus de Teatinos S/N, 29010 Málaga, Spain

ORCID IDs: 0000-0001-8026-1937 (A.L.); 0000-0001-8392-453X (M.C.M.); 0000-0002-8177-9065 (G.G.-M.); 0000-0002-5738-6712 (C.C.-F.); 0000-0002-7747-2722 (L.R.); 0000-0002-3034-8708 (J.A.F.); 0000-0003-1961-5243 (A.-A.V.); 0000-0002-9087-3838 (J.M.M.); 0000-0001-8589-7002 (L.Y.).

Potassium (K^+) is a key monovalent cation necessary for multiple aspects of cell growth and survival. In plants, this cation also plays a key role in the control of stomatal movement. KAT1 and its homolog KAT2 are the main inward rectifying channels present in guard cells, mediating K^+ influx into these cells, resulting in stomatal opening. To gain further insight into the regulation of these channels, we performed a split-ubiquitin protein-protein interaction screen searching for KAT1 interactors in Arabidopsis (*Arabidopsis thaliana*). We characterized one of these candidates, BCL2-ASSOCIATED ATHANOGENE4 (BAG4), in detail using biochemical and genetic approaches to confirm this interaction and its effect on KAT1 activity. We show that BAG4 improves KAT1-mediated K^+ transport in two heterologous systems and provide evidence that in plants, BAG4 interacts with KAT1 and favors the arrival of KAT1 at the plasma membrane. Importantly, lines lacking or overexpressing the *BAG4* gene show altered KAT1 plasma membrane accumulation and alterations in stomatal movement. Our data allowed us to identify a KAT1 regulator and define a potential target for the plant BAG family. The identification of physiologically relevant regulators of K^+ channels will aid in the design of approaches that may impact drought tolerance and pathogen susceptibility.

Ion homeostasis is a dynamic process essential for the normal functioning of any organism. Some minerals are required for biological processes, but their excess or deficiency is deleterious. In addition, cells must discriminate between the physiologically relevant ions and the toxic ions that may be chemically similar. For this reason, all living organisms have developed efficient systems to capture and store ions and complex mechanisms to maintain homeostatic concentrations. In plants, ion homeostasis must provide the environment required to maintain all internal processes, prevent toxicity, and enable the response to environmental changes using the minerals present in the soil.

Potassium is a key monovalent cation necessary for many aspects of growth and survival, among them, compensation of the negative charges generated in processes such as glycolysis, the maintenance of electroneutrality, turgor pressure and cell volume, phloem loading, enzymatic activity, protein synthesis, and the establishment of proper membrane potential and an adequate intracellular pH (Rodríguez-Navarro, 2000).

In plant cells, potassium accumulates to relatively high concentrations in the plant cell cytosol (~100 mM) and in variable amounts in the vacuole (10–200 mM, depending on the tissue and the environmental conditions), while other cations such as sodium must be excluded to avoid toxicity (Pardo and Quintero, 2002). Potassium homeostasis is essential for optimal water use efficiency, as potassium currents participate in stomatal movement. Stomatal opening depends on

[1]This work was supported by the Spanish Ministry of Economy and Competitiveness (BIO201677776-P and BIO2016-81957-REDT) and the Valencian Government (AICO/2018/300).

[2]Author for contact: lynne@ibmcp.upv.es.

[3]Senior author.

The author responsible for distribution of materials integral to the findings presented in this article in accordance with the policy described in the Instructions for Authors (www.plantphysiol.org) is: Lynne Yenush (lynne@ibmcp.upv.es).

A.L., M.C.M,. G.G.-M., N.A.-C., C.C.-F., and L.Y. performed the experiments; L.Y. and J.M.M. designed and supervised the project; L.Y., J.M.M., A.L., L.R., A.-A.V., J.A.F., and C.C.-F. participated in the experimental design and writing of the article.

[OPEN]Articles can be viewed without a subscription.

www.plantphysiol.org/cgi/doi/10.1104/pp.19.00224

potassium and anion uptake coupled to increased proton efflux, while stomatal closing depends on potassium and anion efflux (Lawson and Blatt, 2014). Understanding the molecular mechanisms underlying potassium regulation in guard cells can provide valuable information with applications to the development of new varieties of drought-resistant crops. In response to elevated CO_2, drought may be among the main threats to world food production because of its dramatic impact on agricultural productivity. Optimizing water use efficiency of crops by improving the potassium regulation in the guard cell, and therefore improving transpiration regulation, can directly affect food production under adverse conditions (Wang et al., 2014).

In the model plant Arabidopsis (*Arabidopsis thaliana*), there are three different families of plasma membrane potassium transport systems: the CPA2 subfamily, including the cation/H^+ exchanger and K^+ efflux (KEA) H^+/K^+ antiporters (Mäser et al., 2001); the HAK/KUP/KT K^+ transporters (Gierth and Mäser, 2007); and the Shaker-type K^+ channels (Véry and Sentenac, 2003). The third family, Shaker channels, is present in animals, plants, yeast, and bacteria. The genome of Arabidopsis contains nine members that are classified into five different groups depending on their phylogeny and functional aspects (Pilot et al., 2003). Groups 1 and 2 contain four inward-rectifying channels (AKT1, AKT6, KAT1, and KAT2), while group 3 contains a weak inward rectifier (AKT2). Group 4 contains a "Silent" channel (KC1) and group 5 consists of two outward-rectifying channels (GORK and SKOR). This family of voltage-dependent channels selective for potassium is responsible for the K^+ conductance in the plasma membrane in most cell types. Based on the structural data obtained for bacterial and mammalian Shaker channels, it has been proposed that this family adopts a homo- or heterotetrameric structure that forms the potassium pore (Jiang et al., 2003; Long et al., 2005). For example, AKT1 has been proposed to form functional channels with KC1 and KAT2, while KAT1 and KAT2 can associate with each other and also with KC1 (and AKT2 in the case of KAT2; Lebaudy et al., 2010; Jeanguenin et al., 2011). KC1 is considered a "silent" channel since it is only able to induce currents when it is part of heterotetramers (Dreyer et al., 1997; Duby et al., 2008; Jeanguenin et al., 2011). It is considered that this multiplicity in the composition of subunits confers different properties to the channel, and this would be a reflection of different physiological functions (Ivashikina et al., 2001; Xicluna et al., 2007; Jeanguenin et al., 2011).

Two members of the Shaker family, KAT1 and KAT2, are major contributors to potassium influxes in guard cells (Nakamura et al., 1995; Szyroki et al., 2001; Lebaudy et al., 2008). As potassium homeostasis contributes to the regulation of stomatal movement, this process requires tight regulation, which allows fast activation and inactivation, to prevent excessive water loss, specifically under drought or saline conditions (Lebaudy et al., 2008). Therefore, the identification and characterization of the proteins interacting with the KAT1 potassium channel may provide new insights into potassium homeostasis regulation and new ways to develop drought-tolerant plants.

KAT1 is considered the prototype of inward-rectifying potassium channels and plays an important role in potassium fluxes in the guard cell, as mentioned above (Anderson et al., 1992; Schachtman et al., 1992; Nakamura et al., 1995). Several proteins have been implicated in KAT1 regulation. For example, it has been described that fusicoccin can stabilize the interaction of KAT1 with 14-3-3 proteins and activate its transport activity (Saponaro et al., 2017), but the underlying mechanism of this regulation at the level of protein–protein interaction remains largely unexplored. Previous studies have shown that both the Ost1 (SnRK2.6) and CPK13 kinases can phosphorylate KAT1, although the molecular mechanism by which these phosphorylation events regulate the channel is as yet undefined (Sato et al., 2009; Ronzier et al., 2014). In addition, work from the Blatt laboratory has shown that VAMP721 and SYP121 are important for KAT1 trafficking and gating of the channel (Sutter et al., 2006; Eisenach et al., 2012; Zhang et al., 2015, 2017; Lefoulon et al., 2018). As these channels play an instrumental role in stomatal movement, their regulation is likely to be complex, involving several different classes of regulatory molecules.

In our study, we used a split-ubiquitin approach to identify proteins interacting with KAT1. We found that the BCL2-associated athanogene (BAG) 4 protein interacts with KAT1. BAG4 is a member of an evolutionarily conserved family defined by the presence of the BAG domain. This domain is ~110–125 amino acids long and is composed of three antiparallel α-helices of 30–40 amino acids (Takayama and Reed, 2001). BAG family proteins have been extensively studied in mammalian systems, where they have been shown to regulate several processes, in many cases by recruiting cochaperones and different chaperone systems, including the Heat shock protein 70 (Hsp70), which binds to helices 2 and 3 of the BAG domain (Takayama and Reed, 2001; Kabbage and Dickman, 2008). In plants, BAG proteins have been related to processes such as the unfolded protein response, pathogen resistance, and abiotic stress and have been shown to conserve the ability to bind to Hsp70 (Doukhanina et al., 2006; Williams et al., 2010; Kabbage et al., 2016), although the molecular mechanisms underlying their function are largely undefined. More specifically, overexpression of BAG4 is able to increase salinity tolerance in Arabidopsis and rice (Doukhanina et al., 2006; Hoang et al., 2015), and BAG1 and BAG6 have been implicated in the proteasomal degradation of plastid proteins and fungal resistance, respectively (Kabbage et al., 2016; Lee et al., 2016). In this report, we show that BAG4 expression increases KAT1 activity in both yeast and *Xenopus* oocytes. Moreover, we have confirmed the KAT1-BAG4 interaction in plants and provide evidence that BAG4 plays a role in the arrival of KAT1 at the plasma

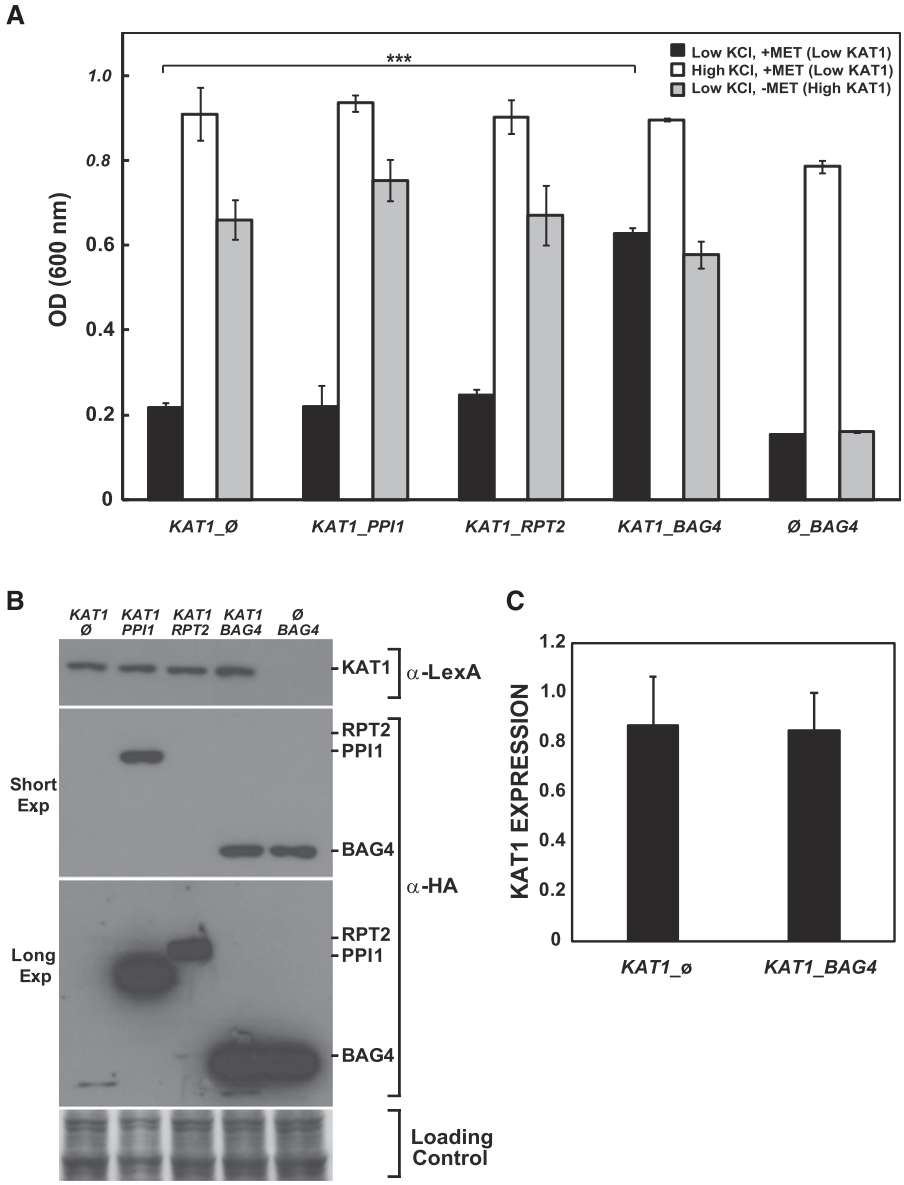

Figure 1. Effect of the coexpression of interacting proteins on functional complementation by KAT1 in yeast. A, The indicated plasmids were cotransformed in the *trk1 trk2* mutant strain (PLY240) and the growth of the strains was assayed as described in "Materials and Methods" using the Translucent media (which contains 12 μM potassium) with or without Met supplementation to decrease the expression of KAT1 (under control of the *MET25* promoter). The graph shows the average value of the optical density at 72 h for triplicate determinations, and the experiment was done with at least three independent transformants for each plasmid combination. Translucent media with no KCl supplementation = Low KCl (12 μM K^+); Translucent media containing 0.75 mg/mL Met = Low KAT1; Translucent media + 50 mM KCl added = High KCl; Translucent media ± KCl without Met = High KAT1). Data are presented as the mean ± SD, and similar results were observed for three independent transformants. Asterisks indicate statistical significance (**$P < 0.01$; Student's *t*-test). B, Immunoblot analysis of protein extracts from the indicated strains, showing the correct expression of each of the fusion proteins. The KAT1 bait vector protein is detected with the anti-LexA antibody (α-LexA) and the prey proteins with the anti-HA antibody (α-HA). Results for a representative clone are shown. The long exposure is included to visualize the expression of the RPT2 prey protein, which accumulates less than the other two prey proteins. C, The KAT1 signal and the corresponding loading control were quantified using ImageJ software and the average values of KAT1/loading control (normalized KAT1) was calculated for six control strains (KAT1_empty vector) and seven KAT1_BAG4 strains. Data are presented as the mean ± SD.

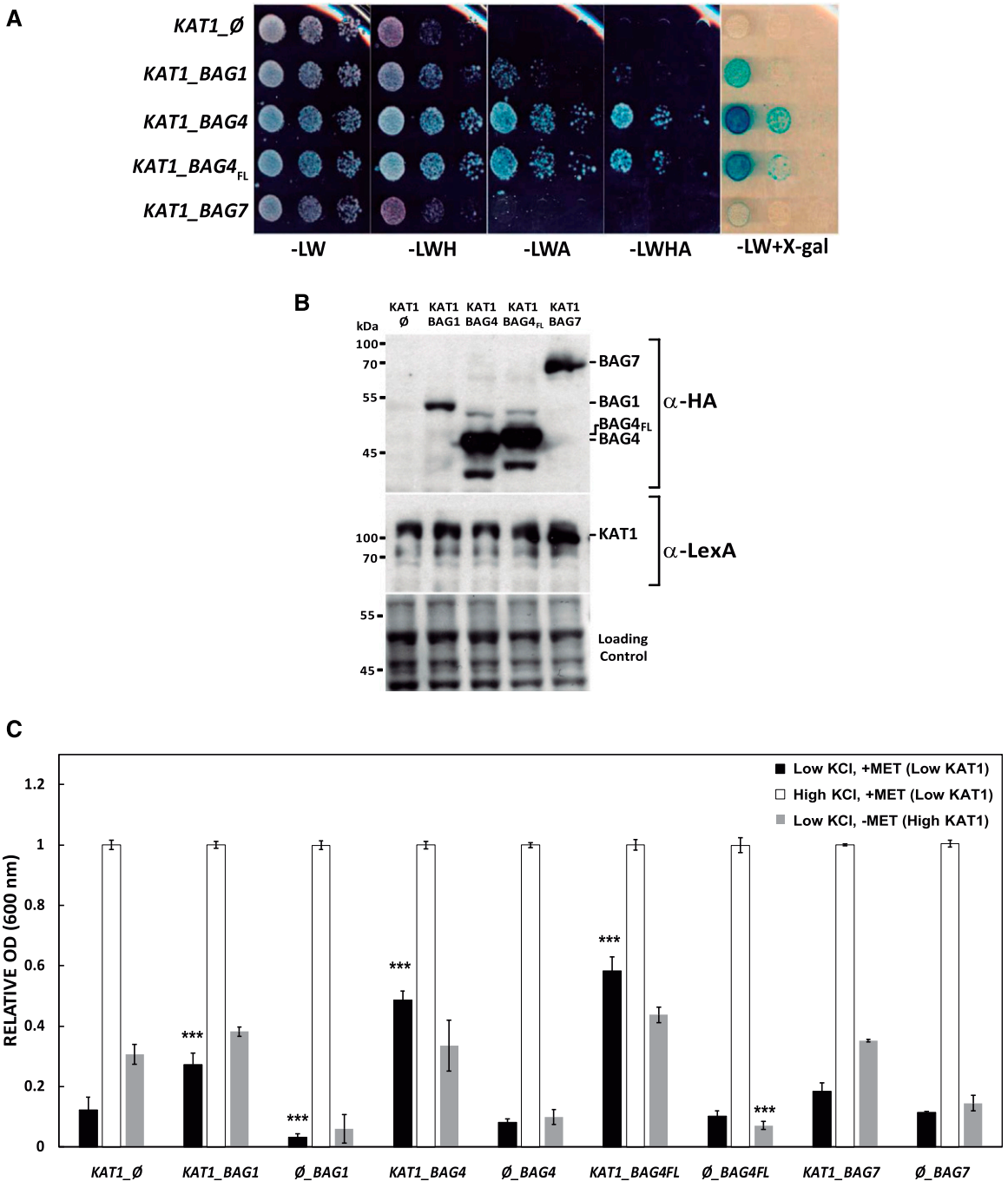

Figure 2. Study of the specificity of the interaction between KAT1 and other BAG family members. A, The indicated plasmids were transformed into the THY.AP4 strain and grown to saturation in selective media. Serial dilutions were spotted onto media with the indicated compositions to test for the protein-protein interaction between KAT1 and the indicated BAG family proteins. Identical results were observed for four independent clones. L, leucine; W, tryptophan; H, histidine; A, adenine; X-gal, 5-bromo-4-chloro-3-indolyl-b-d-galactopyranoside acid. B, Immunoblot analysis of protein extracts from the indicated strains showing the correct expression of each of the fusion proteins. The KAT1 bait protein is detected with the anti-LexA antibody and the prey proteins with the anti-HA antibody. Results for a representative clone are shown. C, The indicated plasmids were cotransformed in the *trk1 trk2* mutant strain (PLY240) and the growth of the strains was assayed as described in Figure 1A. The average value of triplicate determinations of the optical density of the growth normalized to the potassium-supplemented media is shown for each strain. Data are presented as the mean ± SD, and similar results were observed for three independent clones of each plasmid combination. Asterisks indicate statistical significance compared to the KAT1_ø control strain(***$P < 0.001$; Student's *t*-test).

membrane in both gain- and loss-of-function experiments. In addition, mutants lacking or overexpressing the *BAG4* gene present alterations in stomatal opening dynamics, consistent with a physiological role in modulating potassium fluxes. Taken together, our data suggest that in plants, BAG4 acts as a KAT1 regulator. Our work uncovers an important potential client for the plant BAG protein family.

RESULTS

In order to gain further insight into the posttranslational regulation of the KAT1 inward-rectifying potassium channel, we carried out a high-throughput screening for physical interactors using the split-ubiquitin yeast two-hybrid assay with an Arabidopsis complementary DNA (cDNA) library, as described in "Materials and Methods." Previous reports have shown that KAT1 interactions can be detected using this method (Obrdlik et al., 2004). Using this approach, we identified BAG4 as a KAT1 interacting protein.

As a first step in the characterization of this interaction, we carried out a functional complementation assay in yeast for selected candidates. We cotransformed KAT1 with BAG4 and two other candidate proteins into a yeast strain lacking the endogenous high-affinity potassium transporters (Trk1 and Trk2). This strain grows very poorly in media with limiting amounts of potassium (12 μM; Navarrete et al., 2010). However, KAT1 expression functionally complements this phenotype. The plasmid containing the *KAT1* sequence is under control of the *MET25* promoter and in the presence of 0.75 mg/mL Met the expression of *KAT1* is reduced to low levels (Mumberg et al., 1994), providing a sensitive system to study KAT1 activity. In order to determine whether BAG4 could functionally regulate KAT1, we performed growth assays in liquid media under three conditions: (1) low KAT1 expression (Met supplementation) and low potassium (no KCl supplementation); (2) low KAT1 expression and high potassium (50 mM KCl); and (3) high KAT1 expression and low potassium. As shown in Figure 1, coexpression of BAG4 with KAT1 improved growth under limiting potassium conditions, whereas two other Arabidopsis proteins recovered in the screening (proton pump interacting protein 1 [PPI1]) and root phototropism 2 [RPT2]) had no functional effect in this assay. Correct expression of the proteins was confirmed by immunodetection (Fig. 1). As observed, both BAG4 and PPI1 accumulated to similar levels, whereas RPT2 accumulated to lower levels in yeast. This result is consistent with BAG4 improving KAT1 activity in this heterologous system. Based on this phenotype, BAG4 was selected for further analysis. We next wanted to confirm that the increase in growth in this assay was not due to increased expression of the KAT1 protein upon BAG4 overexpression. For this, we determined the levels of KAT1 in six control strains and seven strains coexpressing BAG4. As shown in Figure 1, we observed no change in KAT1 protein levels, suggesting that the effect of BAG4 is not due to increased accumulation of KAT1, and so mechanisms based on transcriptional regulation and protein turnover in this model system can be discarded.

BAG4 belongs to a seven-member family of proteins, all containing a BAG domain (Doukhanina et al., 2006). BAG1 and BAG7 have domain structures similar to that of BAG4 and so were chosen for further analysis. Using the yeast assays described above, we compared both the interaction and the functional complementation between BAG family members. Since the original BAG4 clone recovered from the screening had a 13-amino acid N-terminal truncation, we cloned the full-length *BAG4* gene and included it in these assays. As observed in the split-ubiquitin protein–protein interaction assay shown in Figure 2, we observed the strongest interaction between KAT1 and the BAG4 isoforms, as judged by the growth in selective media and the X-gal plate assay. A moderate interaction was observed for BAG1, whereas the interaction between KAT1 and BAG7 was very weak. The data presented in Figure 2 confirm the proper expression of each of the proteins. The same pattern of relative KAT1-BAG protein interaction (BAG4 $>$ BAG1 $>>$ BAG7) was observed in the functional complementation assay shown in Figure 2. The combinations between KAT1 and the two versions of BAG4 show the highest growth in low-potassium medium when KAT1 is limiting (black bars). Some growth is detected under these conditions upon coexpression of BAG1, but in the presence of BAG7 the level of growth is the same as for the control. Thus, we provide evidence for some level of specificity between KAT1 and BAG family members, lending further support to the possible physiological relevance of the KAT1-BAG4 interaction.

In order to confirm that the observed improvement in growth of the KAT1_BAG4 strain is due to improved potassium uptake, we analyzed potassium uptake using K^+-specific electrodes (see "Materials and Methods" for a complete description). As shown in Figure 3, coexpression of BAG4 increased both the total amount and the initial rate of potassium uptake from the media. As an internal control, we measured the acidification of the media (due to the H^+-ATPase activity) and, as expected, observed no changes in the presence or absence of BAG4 (Fig. 3). These experiments strongly suggest that BAG4 favors KAT1 potassium transport activity, at least in yeast.

Xenopus oocytes have been extensively used to characterize potassium channels from many organisms. We studied the effect of BAG4 coexpression on KAT1-mediated currents in this model system. We observed an increase in KAT1 channel activity 1 d after complementary RNA (cRNA) injection into the oocytes (Fig. 4; Supplemental Fig. S1). At later times (from day 2), when reaching steady-state expression level, no differences in the currents were observed (Supplemental Fig. S1). KAT1 current increase upon BAG4 coexpression 1 d after oocyte injection was 50% to 100% in the

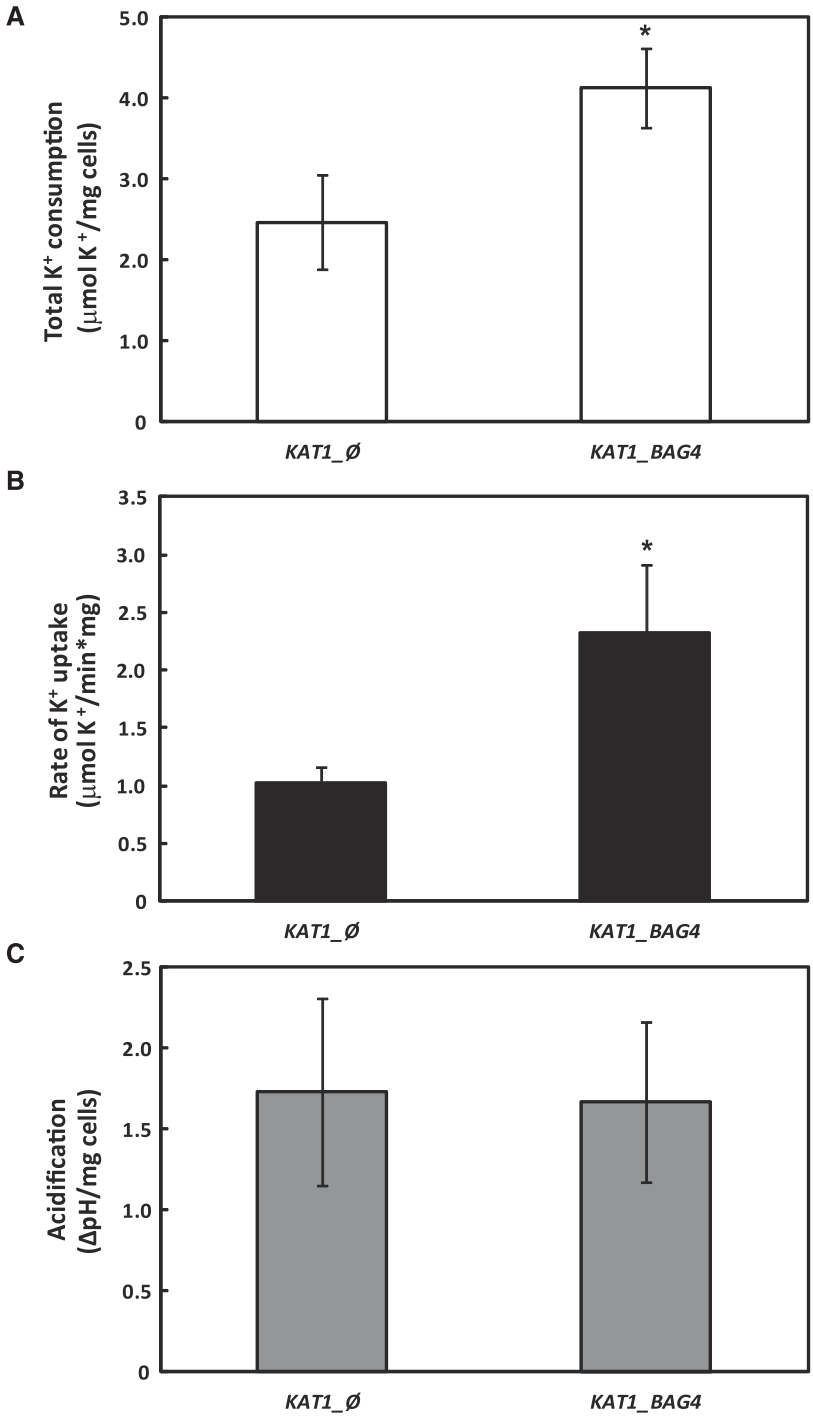

Figure 3. Potassium uptake and external acidification. The indicated plasmids were cotransformed in the *trk1 trk2* mutant strain (PLY240) and the strains were grown in low KCl and low KAT1 conditions and processed as described in "Materials and Methods." A, The bars represent the average value from three independent experiments for the total potassium uptake over 45 min, expressed as μmol K^+/mg cells ± SD. B, The bars represent the average value from three independent experiments for the initial rate of potassium uptake, expressed as μmol K^+/min*mg cells, calculated using the slope of the depletion curve (first 5–18 min) normalized to the wet weight of the cells ± SD. C, The bars represent the average value from three independent experiments for the change in the pH value measured in parallel with the potassium consumption ± SD. The change in the external pH was determined during the first 15 min after Glc addition and was normalized to the wet weight of the cells. Asterisks indicate statistical significance(*$P <$ 0.05; Student's *t*-test).

different experiments at all membrane voltages (Fig. 4; Supplemental Fig. S1). No shift in KAT1 voltage dependence was observed under coexpression (Fig. 4). One interpretation of these results contends that BAG4 coexpression favors the targeting of active KAT1 channels at the oocyte cell membrane, consistent with what is observed in the experiments described above in yeast.

We next wanted to confirm that the interaction between BAG4 and KAT1 also takes place in plants. To this end, we performed both bimolecular fluorescence complementation (BiFC) and coimmunoprecipitation assays in *Nicotiana benthamiana* infiltrated with *Agrobacterium tumefaciens* containing the appropriate plasmids. As a positive control, we used the KAT1-KAT1 interaction (Fig. 5), observing a uniform fluorescent signal at the plasma membrane. By contrast, we observed a punctate signal corresponding to the KAT1-BAG4 interaction but observed no signal for the corresponding control experiments (Fig. 5). In addition,

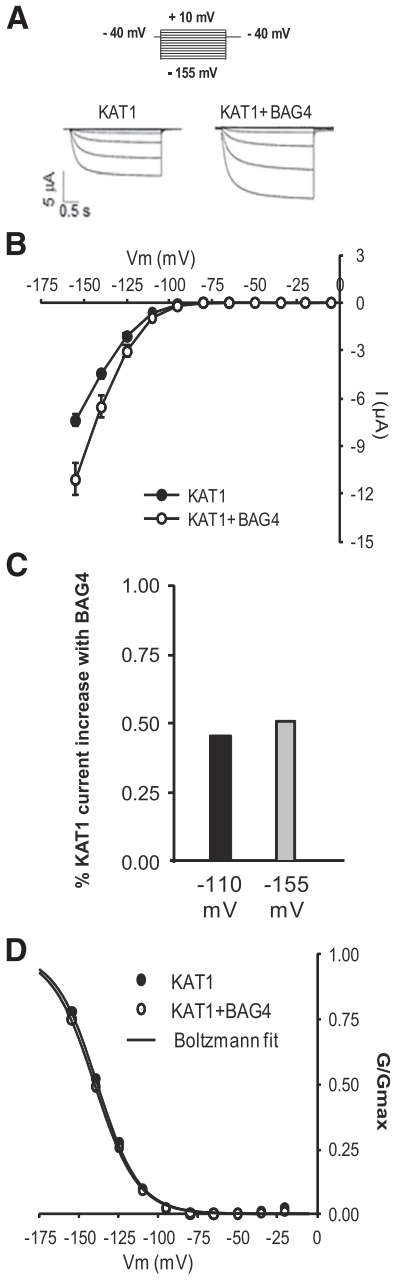

Figure 4. BAG4 coexpression increases the KAT1 current in *Xenopus* oocytes. A, Voltage-clamp protocol and representative current traces recorded by two-electrode voltage clamp in the presence of 100 mM KCl on oocytes coexpressing KAT1 or KAT1 and BAG4. B, KAT1 current (I)-voltage (Vm) relationships of oocytes coexpressing KAT1 and BAG4 (white circles) or KAT1 alone (black circles). Data are means ± SE ($n = 7$ for KAT1, $n = 11$ for KAT1 + BAG4) and are representative of three experiments performed on different oocyte batches. C, Increase of mean KAT1 current upon BAG4 coexpression, at −110 mV (black) and −155 mV (gray). Mean currents are from (B). D, Voltage dependence of KAT1-current activation in the presence of BAG4 (white circles) or expressed alone (black circles). Gating parameters (z, gating charge: 1.95 or 1.9 in absence or presence of BAG4; Ea50, half activation potential: −138 or −140 mV in absence or presence of BAG4) with a Boltzmann function coupled to a linear relation (Lebaudy et al., 2010). G, KAT1 macroscopic conductance (G=I/(Vm-Erev)); Erev, reversal potential of KAT1 currents; G_{max}, KAT1 macroscopic conductance at infinitely negative voltage.

to add experimental support for this interaction in plants, we performed coimmunoprecipitation experiments upon transient expression in *N. benthamiana*. We were able to efficiently recover BAG4 upon KAT1 immunoprecipitation performed in protein extracts obtained from *N. benthamiana* leaves transiently expressing the two proteins (Fig. 5).

We next performed colocalization experiments to determine the subcellular localization of the KAT1-BAG4 complex. We show that the signal corresponding to the KAT1-BAG4 complex colocalizes with an endoplasmic reticulum (ER) marker protein (cherry fluorescent protein [ChFP]-KDEL), thus lending support to the idea that BAG4 could be involved in KAT1 assembly at this organelle (Fig. 6). Pearson and Mander coefficient analyses indicate a strong degree of colocalization between the KAT1-BAG4 BiFC signal and the ER marker (0.75–0.97 and 0.88–0.99, respectively). By contrast, these same parameters for the KAT1-KAT1 BiFC interaction and the same ER marker indicated no colocalization, as expected (Pearson, −0.17 to 0.035; Mander, 0.016–0.024). Since the signal for the complex is punctate and is not observed throughout the ER, we also performed colocalization experiments with the ER exit site (ERES) marker Sec24-monomeric red fluorescent protein (mRFP) and the transmembrane domain of the rat α-2,6-sialyltransferase fused to the ChFP as a Golgi marker (STtmd-ChFP). We observed colocalization of the KAT1-BAG4 complex with the ERES marker (Pearson, 0.43–0.82; Mander, 0.5–0.98), but not the Golgi marker (Pearson, −0.0039 to 0.042; Mander, 0.1–0.5).

Interestingly, KAT1 was previously shown to interact with Sec24 through its diacidic ER export signal motif (Sieben et al., 2008). Thus, our data confirm the interaction between BAG4 and KAT1 in a plant model system and show that the KAT1-BAG4 interaction likely takes place at the ERES, possibly facilitating its incorporation in coat protein complex II (COPII) vesicles. This is not unexpected, as KAT1, like essentially all multispan plasma membrane proteins, before arriving to the cell surface transits through the ER, where the protein is thought to be assembled into tetramers to form a functional channel that will be inserted into the plasma membrane via the secretory pathway. Our data suggest that BAG4 interacts with KAT1 as it transits through this organelle on its way to the plasma membrane. This model is consistent with that proposed for mammalian BAG proteins that are involved in the regulation of potassium and chloride channels that also act at the ER in cooperation with Hsp70 (Knapp et al., 2014; Hantouche et al., 2017).

Our results indicate that BAG4 favors KAT1 activity in yeast and oocytes and that the interaction appears to take place at the ERESs. We hypothesized that BAG4 acts to facilitate KAT1 transit out of the ER and thus

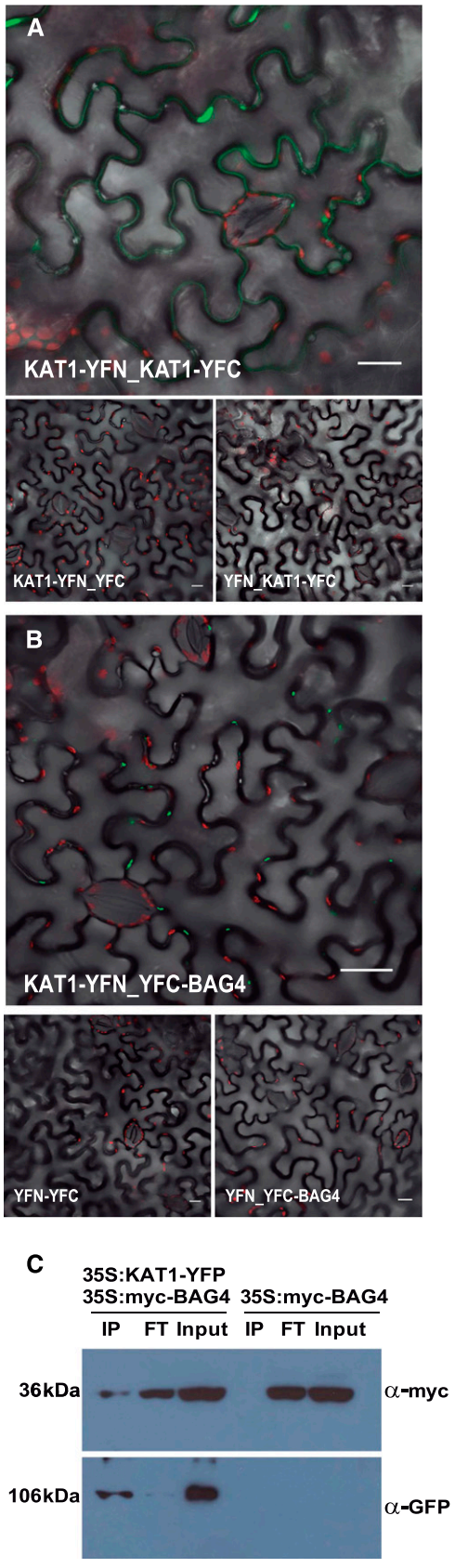

would promote the arrival of active KAT1 channels at the plasma membrane. In order to test this model, we examined whether BAG4 influences the arrival of this channel at the plasma membrane. Our first approach was to observe the time course of KAT1 plasma membrane accumulation in the presence and absence of coexpression of BAG4 in *N. benthamiana*. As shown in Figure 7, when BAG4 is coexpressed, a higher percentage of KAT1 protein is present at the plasma membrane on day 1 after infiltration, whereas in the absence of BAG4, KAT1 accumulation at the plasma membrane is not comparable to that observed for KAT1_BAG4 until day 3. Figure 7 shows representative images on each day with sufficient signal to clearly visualize KAT1 distribution and the quantification of the percentage of the total KAT1-yellow fluorescent protein (YFP) signal present at the plasma membrane for each condition and time point (n = 10 cells). This result is consistent with ectopic BAG4 expression facilitating the assembly of KAT1 containing tetramers and/or their delivery to the plasma membrane, which would in turn favor the accumulation of active channels at the plasma membrane. Since both the yeast and oocyte experiments suggest that BAG4 does not affect overall KAT1 protein accumulation, we tested whether this was also the case in this plant model system. As described in "Materials and Methods," for these transient expression experiments we constructed vectors containing multiple transcriptional units, including an internal control for infiltration efficiency (dsRED containing a human influenza hemagglutinin [HA] tag) within the same plasmid. Plants were agroinfiltrated with strains containing KAT1-YFP:dsRED-HA alone or KAT1-YFP:dsRED-HA:BAG4-myc. We analyzed the amount of KAT1-YFP and the internal control (dsRED-HA) in the infiltrated areas using the same time course. As shown in Figure 7, BAG4 coexpression does not

Figure 5. Confirmation of the interaction between KAT1 and BAG4 in *N. benthamiana*. *Agrobacterium* strains harboring the indicated plasmids were used to infiltrate *N. benthamiana* leaves, and images were obtained using fluorescence confocal microscopy 72 h postinfiltration. A, Representative BiFC images for the KAT1-KAT1 interaction and control plasmids. The overlay of the grayscale and BiFC fluorescence is shown. Leaf epithelial cells and stomata are visible. B, Representative BiFC images for the KAT1-BAG4 interaction. Representative images of the experiments performed with the control plasmids are shown below. The red signal corresponds to chloroplast autofluorescence. For A and B, similar results were observed in at least four independent experiments performed on different days. Bars = 20 μm. C, *Agrobacterium* strains expressing the indicated plasmids were used to infiltrate *N. benthamiana* leaves. Samples were taken at 72 h postinfiltration and processed for protein extraction and coimmunoprecipitation as described in "Materials and Methods." The figure shows the results of the immunodetection using antibodies that recognize the BAG4 and KAT1 proteins. The amount of BAG4 recovered in the KAT1 purification is shown in the first lane on the left. Similar results were observed in two independent experiments performed on different days. FT = flow-through; IP, immunoprecipitation; YFC, C-terminal part of YFP ; YFN, N-terminal part of YFP.

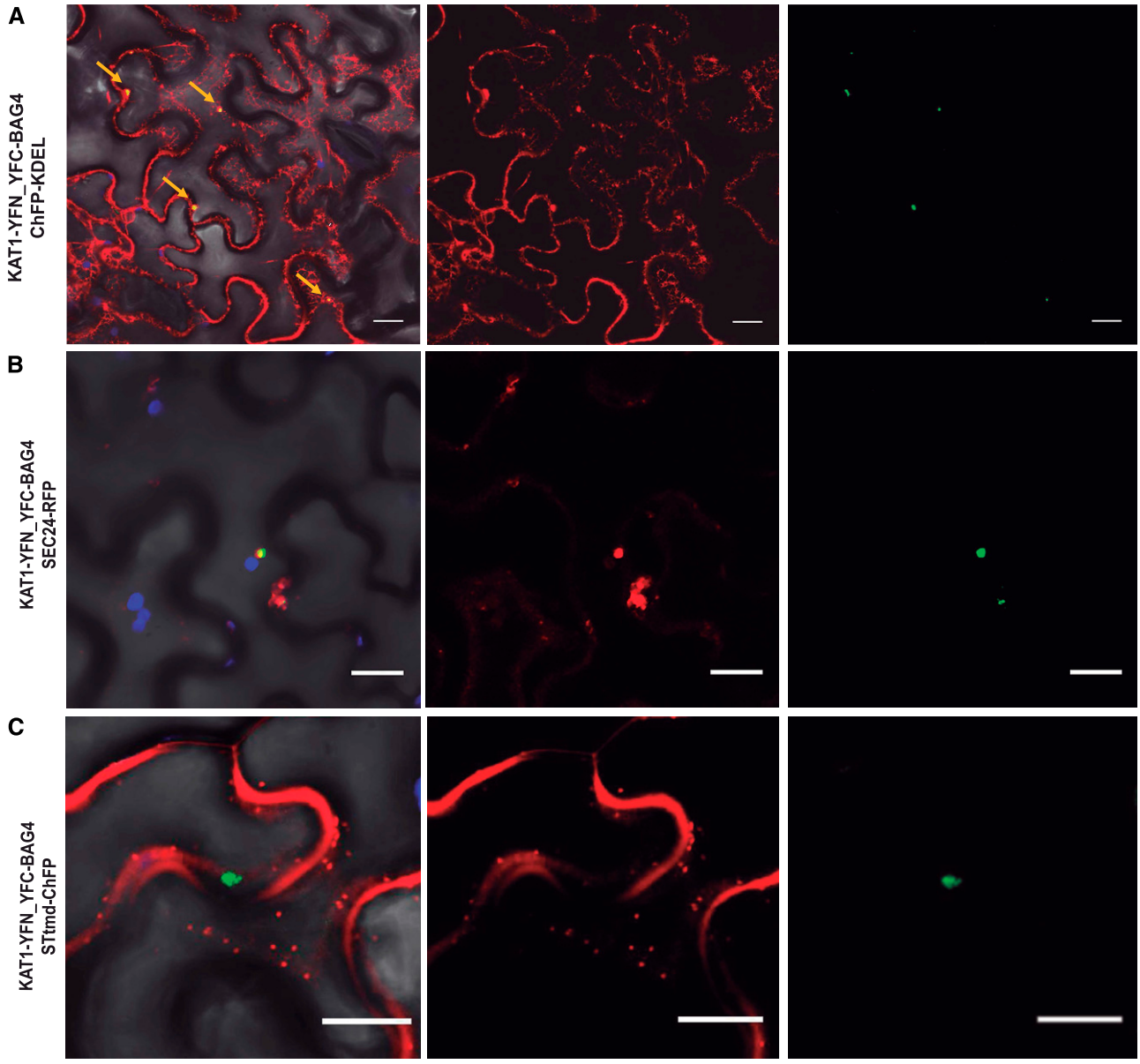

Figure 6. The KAT1-BAG4 complex colocalizes with the ER and ERES markers. A, A plasmid containing the KAT1-BAG4 BiFC interaction and the ER marker ChFP-KDEL was infiltrated as described. The BiFC signal (right), ChFP signal (center), and overlay image of the grayscale, BiFC fluorescence, and ChFP signals (left) are shown. Leaf epithelial cells and stomata are visible. B and C, The same colocalization analysis of the KAT1-BAG4 complex was performed with the ERES marker Sec24 fused to RFP (Sec24-RFP; B) and the STtmd-ChFP Golgi marker (C). The yellow arrows (A) indicate the points of colocalization with the ER marker. Chloroplast autofluorescence is shown in blue (B). Bars = 20μm. STtmd-ChFP = rat α-2,6-sialyltransferase transmembrane domain fused to ChFP ; YFC, C-terminal part of YFP; YFN, N-terminal part of YFP .

increase the steady-state amount of KAT1 protein. So, taken together, the data presented in Figure 7 clearly suggest that expression of BAG4 promotes KAT1-YFP arrival at the plasma membrane.

In order to corroborate these observations, we carried out the opposite approach. We investigated the localization of KAT1 in Col-0 wild-type plants and *bag4* mutant lines using transient expression in Arabidopsis (Fig. 7). Employing the AGROBEST transient transformation protocol (Wu et al., 2014), we observed KAT1 accumulation at the plasma membrane in wild-type control plants. However, under the same conditions, in *bag4* mutants, the KAT1 signal observed at the cell surface was markedly decreased and an accumulation of punctate staining was observed (Fig. 7). We could complement this defect of KAT1 plasma membrane targeting observed in the *bag4* mutant by employing vectors coexpressing BAG4 with KAT1. Figure 7 also shows the quantification of the percentage of the total KAT1 signal present at the plasma membrane for each

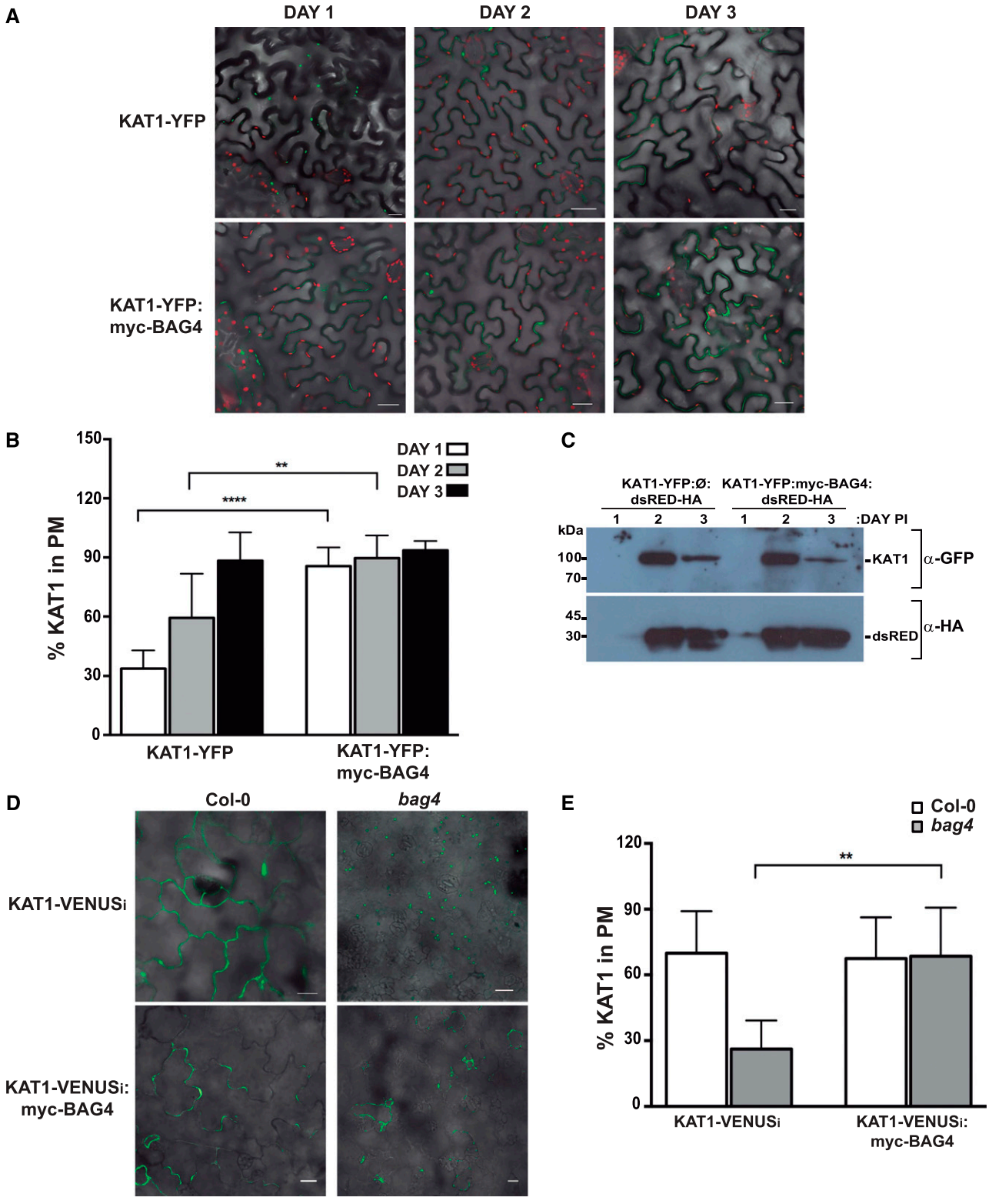

Figure 7. BAG4 expression effects the subcellular localization of KAT1. A, Plasmids containing KAT1-YFP or both KAT1-YFP and BAG4 were transiently expressed in *N. benthamiana* using agro-infiltration. The fluorescence signal was analyzed by confocal microscopy at 1, 2, and 3 d postinfiltration. Representative images are shown. Leaf epithelial cells and stomata are visible. Similar results were observed in three independent experiments performed on different days. Bars = 20μm. B, The percentage of the fluorescence signal present in the plasma membrane (PM) was quantified using ImageJ, as described in "Materials and Methods." The graph shows the average values ± SD for 10 cells for each condition tested. C, Experiments similar to the one described (A)

condition tested ($n = 10$). We observed a much lower percentage of KAT1-YFP at the plasma membrane in *bag4* mutants, as compared to the Col-0 control. Moreover, KAT1-YFP plasma membrane localization is recovered when we functionally complement the *bag4* mutant. These results support the previous experiments and suggest that the presence of BAG4 promotes the arrival of KAT1 at the plasma membrane, possibly by facilitating its assembly and/or delivery to the cell surface, likely through their physical interaction at the ERESs.

In order to provide additional evidence showing that BAG4 is a physiologically relevant KAT1 regulator, we analyzed phenotypes related to KAT1 activity in Arabidopsis lines lacking or overexpressing the *BAG4* gene. Two independent *bag4* mutant lines and two Col-0 lines and one *kat1* line overexpressing *BAG4* were tested for stomatal opening dynamics. The *kat1* and *kat2* single mutants and the *kat1 kat2* double mutant were included for comparison. As shown in Figure 8, two mutant lines lacking the *BAG4* gene show a delay in stomatal opening under all conditions tested. We also observed an initial delay in stomatal opening in the *kat1* and *kat2* mutant lines in response to light treatment, but not potassium-containing opening buffer. Therefore, at high potassium concentrations, the single mutants are able to open their stomata, likely due to the redundancy of inward-rectifying potassium channels. This idea is supported by the phenotype observed for the *kat1 kat2* double mutant, which shows a marked delay in both light and opening buffer. On the other hand, we observed that the overexpression of *BAG4* in Col-0 leads to an increase in stomatal aperture and this response is attenuated in the *kat1* mutant overexpressing *BAG4* (Fig. 8). The levels of expression of the BAG4 protein are shown in Supplemental Figure S2.

As a complementary approach, we measured the temperature of the different mutants and BAG4 gain- and loss-of-function lines using infrared thermography (Fig. 9). Several studies have shown that this technique can be used for analyzing mutants with altered stomatal function because a relationship exists between the temperature of the leaves and variations in stomatal conductance (Jones, 1999; Merlot et al., 2002; Wang et al., 2004). We observed the expected increase in temperature in the lines that showed delayed stomatal aperture dynamics and a decrease in temperature in the Col-0 lines overexpressing BAG4 (Fig. 9). When these results are considered together, they strongly suggest that BAG4 plays a physiologically relevant role in regulating potassium fluxes in stomata and possibly other cells. Importantly, the *BAG4* gene has been reported to be expressed in guard cells, which is a prerequisite for a physiologically relevant KAT1 regulator (Yang et al., 2008).

As discussed above, in the stomatal response assay, we observed additional phenotypes in the *bag4* mutant lines, as compared to the *kat1* or *kat2* single mutants. These data suggest that BAG4 may regulate proteins in addition to KAT1, including other potassium channels, like KAT2. Lebaudy and collaborators showed the importance of the guard cell membrane inward-rectifying K^+ channel (GCK_{in}) activity in stomatal movement (Lebaudy et al., 2008), identifying KAT1 and KAT2 as the major contributors. Therefore, we studied whether BAG4 could interact with KAT2 in a BiFC assay in *N. benthamiana*. As shown in Figure 10, we observed a pattern of fluorescence very similar to that observed for the KAT1-BAG4 interaction, but observed no signal in the control combinations. We used the KAT2-KAT1 interaction as a positive control for these assays, showing a uniform interaction at the plasma membrane, similar to what we observed with the KAT1-KAT1 interaction (Fig. 5), confirming the functionality of the KAT2 BiFC fusion. Although further studies are required to characterize the molecular details of these interactions and ascertain whether there are additional targets, our data suggest that BAG4 may act as a regulator of at least these two potassium channels and provide a plausible explanation for the results obtained in the stomatal response assays described.

DISCUSSION

The regulation of ion fluxes in guard cells is crucial for stomatal movement, which is an important determinant of the plant's response to fluctuating environmental conditions (Lebaudy et al., 2008). Inward-rectifying potassium channels are known to play important roles in this process. As such, these channels are predicted to be highly regulated, and as expected, several proteins have been identified as regulators of the KAT1 channel (Sottocornola et al., 2006, 2008; Sato et al., 2009; Eisenach et al., 2012; Ronzier et al., 2014; Zhang et al., 2015; Saponaro et al., 2017). In this report, we describe the identification and initial characterization of a KAT1 regulator that we recovered in a

Figure 7. (*Continued.*)
were performed, but using GoldenBraid plasmids containing KAT1-YFP:dsRED-HA or KAT1-YFP:myc-BAG4:dsRED-HA. Whole-cell extracts were prepared from infiltrated areas (previously confirmed to express KAT1-YFP) and proteins were processed for immunodetection. The dsRED-HA protein serves as an internal control for the efficiency of transient expression. DAY PI, Days postinfiltration. D, The KAT1-$VENUS_{intron}$ (KAT1-$VENUS_i$, top row) and the KAT1-$VENUS_{intron}$–BAG4 (bottom) plasmids were transiently expressed in the Col-0 and the *bag4* mutant Arabidopsis lines using agro-infiltration. The fluorescence signal was analyzed by confocal microscopy 2 d after infiltration. Representative images are shown, and similar results were observed in three independent experiments. Leaf epithelial cells and stomata are visible. Bars = 20μm. E, The percentage of the fluorescence signal present in the PM was quantified using ImageJ, as described in "Materials and Methods." The graph shows the average values ± SD for 10 cells for each condition tested (**$P < 0.01$; Student's *t*-test).

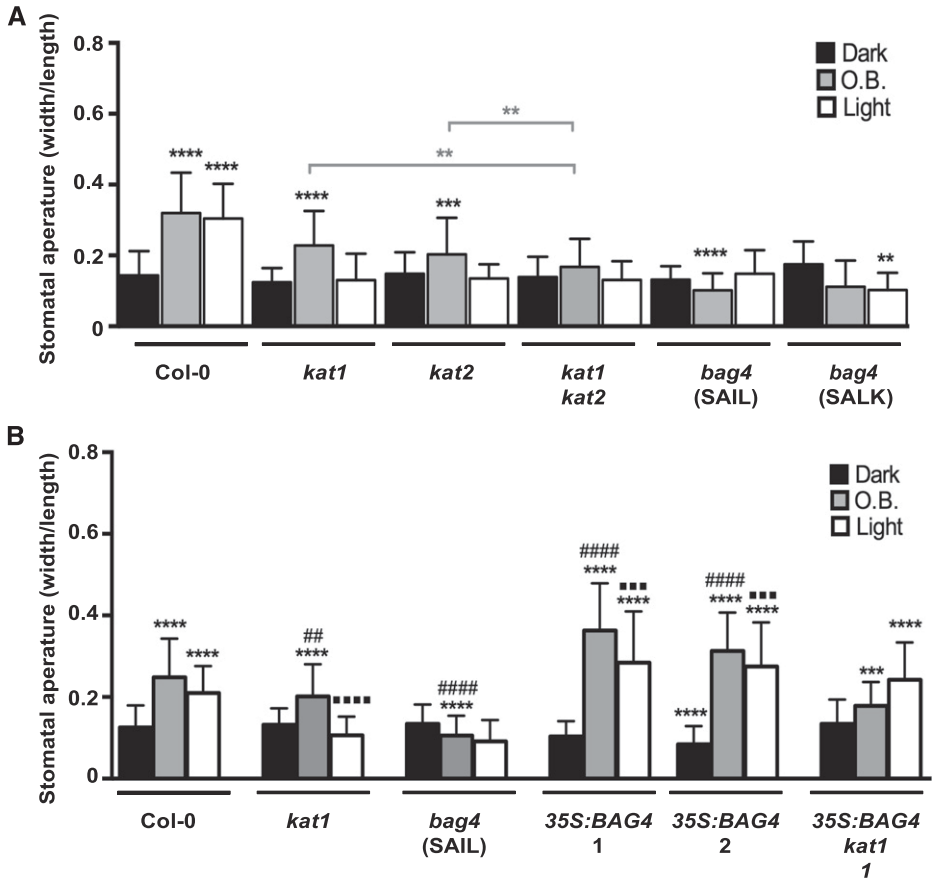

Figure 8. Effect of BAG4 loss and gain of function on stomatal aperture. Stomata from the indicated Arabidopsis lines were analyzed as described in "Materials and Methods." The data show the average ratio ± SD for 60–100 stomata. A, The width/length ratio of stomata of the different mutant lines were determined in leaves from the indicated lines harvested 1 h before the lights turned on (Dark), incubated for 2.5 h in opening buffer in the dark (O.B.) or 2.5 h after the lights turned on (Light). Similar results were observed in three independent experiments. B, The width/length ratio of stomata of control lines and Col-0 and *kat1* homozygous for the 35S:*BAG4* transgene were determined as described in A. For both experiments, the asterisks indicate statistical significance as compared to the Col-0 Dark control (**$P < 0.01$; ***$P < 0.001$; ****$P < 0.0001$; Student's *t*-test). The length/width ratio was also significantly increased in *BAG4* overexpressing lines in both light and opening buffer (# indicates statistical comparison with Col-0 O.B. and ■ indicates statistical comparison with Col-0 Light).

split-ubiquitin screening in yeast. The BAG4 protein was found to physically interact with KAT1 and also to increase potassium uptake in yeast. In oocytes, a similar phenomenon was observed, as increased KAT1 currents were observed 1 d after injection. Thus, our data clearly indicate that in two heterologous systems, BAG4 coexpression increases KAT1 transport activity, likely by increasing the number of active channels at the membrane. It is very unlikely that this regulation is at the transcriptional level in these model organisms, since we could show that the total amount of KAT1 does not change upon BAG4 coexpression in yeast, and in the oocyte experiments, the same amount of KAT1 cRNA is injected in both cases.

We provide experimental evidence for the physical interaction between KAT1 and BAG4 in plants using two complementary approaches, BiFC and coimmunoprecipitation. The signal corresponding to the KAT1-BAG4 complex colocalizes with a general ER marker and with an ERES marker, which supports the notion that BAG4 could be involved in KAT1 assembly at this organelle. BAG4 is a member of a highly conserved family of proteins that all contain a characteristic BAG domain. This domain has been shown to interact with the Hsp70 chaperone in both mammals and plants (Takayama and Reed, 2001; Doukhanina et al., 2006; Kabbage and Dickman, 2008; Lee et al., 2016). On the other hand, Hsp70 has been shown to be required for the assembly of the mammalian potassium channel, hERG1, at the ER (Li et al., 2017). Given the role for the BAG proteins documented in mammals and our observations in yeast and oocytes, we hypothesized that BAG4 may be implicated in the arrival of KAT1 at the plasma membrane, likely at the level of protein folding, tetramer assembly, and/or trafficking. We provide experimental evidence supporting this idea using both gain- and loss-of-function experiments, where we observe an improvement in KAT1 arrival at the plasma membrane upon BAG4 expression and a delay in its accumulation at the plasma membrane in lines lacking the *BAG4* gene. Importantly, we show that the total amount of KAT1 is not affected by BAG4 coexpression, but the percentage of KAT1 that arrives at the plasma membrane is increased. Taken together, these data suggest that the modulation of a step required for KAT1 channel assembly, ER exit, and/or plasma membrane delivery may be one of the functions of the BAG4 protein.

Several studies have addressed KAT1 trafficking and its regulation. For example, efficient transport of KAT1 to the plasma membrane is mediated by a diacidic ER export signal in the C terminus of the protein, which binds to the Sec24 component of coat protein complex II (COPII; Hurst et al., 2004; Meckel et al., 2004; Sieben et al., 2008). Here, we observed the colocalization of the KAT1-BAG4 complex with Sec24, which has been

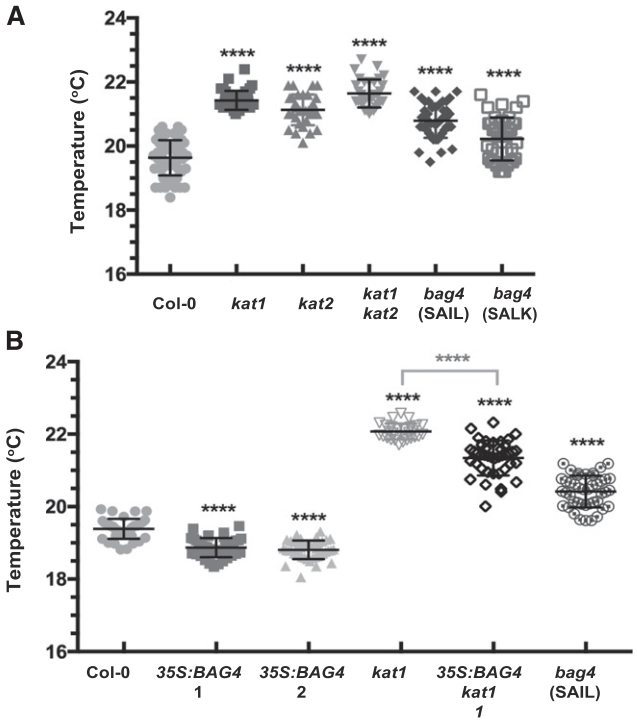

Figure 9. Effect of BAG4 loss and gain of function on leaf temperature. The same lines described in Figure 8 were analyzed for leaf temperature using infrared thermography, as described in "Materials and Methods," for mutant lines (A) and 35S:*BAG4* lines (B). Each symbol represents an individual measurement and the horizontal bar represents the average value for 10 measurements of six different plants for each genotype. The error bars represent the SD. For both experiments, black asterisks indicate statistical significance as compared to the Col-0 control. The gray asterisks and bracket in B indicate comparison between *kat1* and 35S:BAG4 *kat1* (**$P < 0.01$; ***$P < 0.001$; ****$P < 0.0001$; Student's *t*-test).

described as a marker of ER exit sites (for review, see Matheson et al., 2006; Langhans et al., 2012). Therefore, BAG4 may regulate this step of KAT1 processing as it moves out of the ER through the secretory pathway toward the plasma membrane. It has also been shown that abscisic acid stimulates the endocytosis of KAT1 in both epidermal and guard cells, which can then recycle back to the plasma membrane when the levels of the hormone decrease (Sutter et al., 2007). In addition, two trafficking-related proteins, SYP121 and VAMP721, are involved in regulating KAT1 delivery and recycling and more recently have been shown to regulate channel gating (Sutter et al., 2006; Eisenach et al., 2012; Zhang et al., 2015, 2017; Lefoulon et al., 2018). Whether BAG4 is related to any of these known regulatory mechanisms is an interesting question for future studies.

In plants, there are seven members of the BAG family and different phenotypes have been attributed to the *bag1*, *bag4*, and *bag6* loss-of-function mutants, suggesting that each family member may carry out distinct functions (Doukhanina et al., 2006; Kabbage et al., 2016; Lee et al., 2016). Moreover, high-throughput studies have indicated that, for example, both *BAG4* and *BAG1* are expressed in guard cells, whereas *BAG7* expression is low in this cell type (Winter et al., 2007). In order to study the specificity of the KAT1-BAG4 interaction, we used the split-ubiquitin and functional complementation assays to test whether two other BAG family members that share similar domain architecture, BAG1 and BAG7, interacted with KAT1. Our results show that BAG1, the BAG protein with a higher level of conservation compared to BAG4, showed a lower but detectable level of interaction and regulation of KAT1 in yeast. However, a negligible level of interaction was observed for the more distantly related BAG7 protein, thus suggesting a considerable level of specificity for the KAT1-BAG4 interaction.

In order to begin to establish BAG4 as a bona fide KAT1 regulator, we tested whether BAG4 may play a role in a physiological response in which this channel is implicated. Indeed, we observed a delay in stomatal aperture in two independent *bag4* mutant lines in response to external potassium and light. We observed a similar delay in stomatal aperture in response to light in the *kat1* and *kat2* mutant lines. Our data regarding the *kat1* mutant are in contrast to a previous report (Szyroki et al., 2001), but may be explained by differences in the time course studied and/or the mutant lines used. The line used here contains a transfer DNA (T-DNA) insertion in the first exon. In addition, we observed an increase in stomatal aperture in Col-0 lines overexpressing *BAG4*, and this response was reduced when the gene was overexpressed in a *kat1* mutant line. Thus,

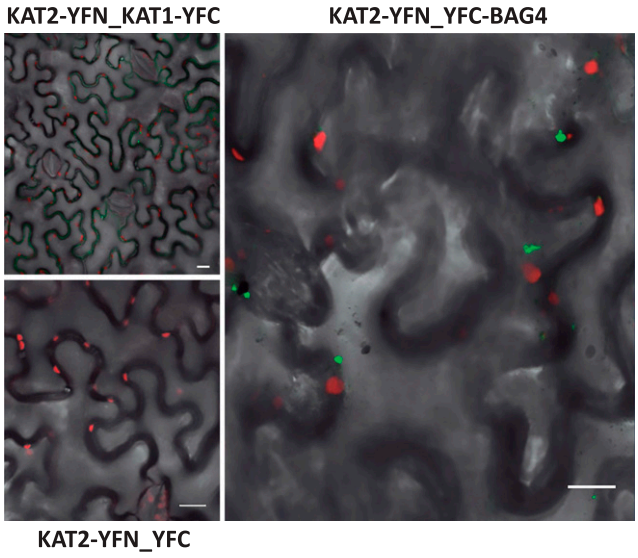

Figure 10. BAG4 interacts with KAT2 in BiFC assays in *N. benthamiana*. Interaction assays were carried out and analyzed as described in Figure 5. Leaf epithelial cells and stomata are visible. As shown, a similar pattern of interaction is observed for KAT2 when tested with BAG4 (compare with Fig. 5B). The BiFC signals corresponding to the KAT2-KAT1 and KAT2-BAG4 interactions are shown in green and the chloroplast autofluorescence is shown in red. YFC, C-terminal part of YFP ; YFN, N-terminal part of YFP. Bars = 20 μm.

we were able to show that both loss- and gain-of-function of *BAG4* affects stomatal aperture dynamics, and that in the case of *BAG4* overexpression, *KAT1* is required to observe the full response.

We corroborated these results by measuring the temperature of the plants as an indirect measure of the transpiration rate. If the stomatal aperture is decreased in *bag4* mutants, so is the rate of transpiration, and therefore, the temperature of the leaves of these plants would be expected to be higher. Our results show that lines lacking the *BAG4* gene display an increased temperature, again adding support to its role in regulating ion fluxes important for stomatal movement. As expected, double mutants lacking both the *KAT1* and *KAT2* genes have a more pronounced phenotype. Moreover, Col-0 lines overexpressing *BAG4* display lower leaf temperatures, which is in agreement with the data regarding stomatal aperture. Taken together, our results establish a role for BAG4 in the regulation of stomatal aperture dynamics through the regulation of the KAT1 inward-rectifying potassium channel.

It is interesting to note that the two *bag4* mutant lines showed a longer delay in stomatal opening in response to opening buffer, which was not observed in the *kat1* and *kat2* single mutants but was observed in the *kat1 kat2* double mutant. BAG proteins are very likely to regulate many different proteins, and in terms of stomatal aperture, other inward-rectifying potassium channels, like KAT2, AKT1, and AKT2/3, are known to contribute to this response. Our genetic data suggest a role for KAT2 as well. To further explore this possibility, we tested whether BAG4 could also interact with KAT2 in plants. Our results using the BiFC assay show a KAT2-BAG4 interaction. Thus, it appears that BAG4 regulates both KAT1 and KAT2, but we cannot rule out other channels as additional targets at this stage.

In mammalian systems, although BAG proteins have been related to many cellular processes, a specific role for BAG proteins in the regulation of ion channels has been reported. Both BAG1 and BAG2 have been shown to regulate the cystic fibrosis transmembrane conductance regulator chloride channel, and BAG1 was more recently implicated in human Ether-à-go-go-related gene (hERG) potassium channel regulation (Young, 2014; Hantouche et al., 2017). In both cases, it appears that the BAG proteins mediate the misfolded protein response, thus likely playing a role in channel degradation, not plasma membrane delivery. Further experiments will be required to clarify the molecular mechanisms responsible for this apparent difference observed here for the plant BAG4 protein. The Arabidopsis BAG1 protein has been reported to be a cofactor in Hsc70-mediated proteasomal degradation of unimported plastid proteins, and so may have a function more analogous to those of its mammalian counterparts (Lee et al., 2016). However, our results identify BAG4 as a positive regulator of the KAT1 (and likely KAT2) potassium channel in plants and thus open a novel line of investigation by linking the plant BAG family to the regulation of potassium channels and stomatal movement.

CONCLUSION

Taken together, the data presented here suggest that one main role for BAG4 in plants may be related to the posttranslational regulation of ion channels and, consequently, stomatal movement. Thus, BAG4 may constitute a novel target for the design of engineered crops with altered potassium fluxes and, concomitantly, improved water use efficiency and drought tolerance.

MATERIALS AND METHODS

Plant Materials and Plant Growth

The following Arabidopsis (*Arabidopsis thaliana*) lines were employed: the *kat1* mutant (SALK 093506, carrying the T-DNA insertion in the first exon), the *kat2* mutant (SALK 025933), and two *bag4* mutant lines, SAIL_144_A10 (carrying the T-DNA insertion in the first exon) and SALK_033845 (carrying the T-DNA insertion in the second exon; obtained from the Salk Institute Genomic Analysis Laboratory and Sessions et al. (2002). Arabidopsis plants were grown under an 8 h light/16 h dark photoperiod at 22°C in Murashige and Skoog media supplemented with 1% (w/v) Suc. For stomatal movement and leaf temperature assays, after 2 weeks, plants were transplanted to soil and analyzed at 4–6 weeks. *Nicotiana benthamiana* plants were grown for 4–5 weeks in soil under a 16 h light/8 h dark photoperiod at 24°C.

Yeast Strains and Plasmids

The split-ubiquitin KAT1 bait vector used for the screening was derived from the KAT1-pMetYCgate vector (ABRC CD3-815; Obrdlik et al., 2004). In order to carry out the screening, the ampicilin resistance gene of the KAT1-pMetYCgate plasmid was substituted with the kanamycin resistance gene (KAN^r) by recombination in yeast as follows: the KAN^r gene was amplified with the primers Kan-F 5′-ttcttgaagacgaaagggcctcgtgatacgcctattTCCAGTTCG ATTTATTC AACAAAG-3′ and Kan-R 5′-taaagtatatatgagtaaacttggtctgacagttac GATCGATCCTAG TAAGCCACGTTG-3′ and was cotransformed in the PLY240 strain (MATa *his3*Δ200 *leu2*-3,112 *trp1*Δ901 *ura3*-52 *suc2*Δ9 *trk1*Δ51 *trk2*Δ50::lox-KanMX-lox; Bertl et al., 2003) together with the KAT1-pMETYCgate vector linearized with AatII. Clones growing in media lacking Leu were tested for growth in media containing 50 mM LiCl to select strains expressing KAT1. Plasmids were recovered from these yeast strains and transformed into DH5α and kanamycin-resistant colonies were selected. The resulting plasmid was confirmed by sequencing. The cDNA library from 6-d-old Arabidopsis seedlings in the pDSL-Nx vector was obtained from Dualsystems Biotech AG. The screening was carried out in the THY.AP4 strain (MATa, *ura3*, *leu2*, lexA::lacZ::*trp1*, lexA::*HIS3*, lexA::*ADE2*; Paumi et al., 2007). The BAG4 clone recovered in the screening lacks the sequence encoding the first 13 amino acids. The BAG1, BAG7, and full-length BAG4 plasmids were constructed by recombination into the pDSL-Nx vector in yeast using PCR products amplified from a cDNA library made from Arabidopsis seedlings.

Split-Ubiquitin Screening

The THY.AP4 strain containing the modified KAT1-Cub (KAT1-CubKAN^r) plasmid was transformed with 20 μg of the Arabidopsis cDNA library in the pDLSN-X vector (Dualsystems Biotech). Approximately 8.6×10^6 transformants were analyzed for growth in selective media. The first 125 colonies growing in selective media were analyzed. Plasmids were recovered, retransformed, tested for growth in selective media, classified by restriction analysis, and subjected to specificity tests using the Ost3-Cub vector encoding a yeast oligosaccharyl transferase (Yan et al., 2005). The clones that passed these tests were then sequenced and analyzed in the yeast functional complementation assay.

Functional Complementation Assay in Yeast

The PLY240 strain was cotransformed with the KAT1-CubKAN^r and the indicated pDLSN-X vectors and the empty vector corresponding controls. Precultures were grown to saturation in synthetic dextrose media supplemented

with auxotrophic requirements, 0.75 mg/mL Met (to reduce KAT1 expression), and 0.1 M KCl. Fresh cultures (1:20 dilution) were grown for 16 h in low-potassium translucent media supplemented with requirements and Met (For-Medium; Navarrete et al., 2010) and diluted to OD_{600} 0.2 in three different conditions of Translucent media supplemented with auxotrophic requirements: (1) low potassium, no Met (low KCl, high KAT1 expression); (2) low potassium, 0.75 mg/mL Met (low KCl, low KAT1 expression); and (3) 0.1 M KCl, no Met (high KCl, high *KAT1* expression). The Translucent medium contains 12 μM K^+. The optical density was determined periodically for 72 h using a BioscreenC system (Oy Growth Curves Ab Ltd). Triplicate determinations were performed for at least three independent transformants for each plasmid combination. Similar results were observed in all experiments. Correct expression of each fusion protein was confirmed by immunoblot analysis of the corresponding whole-cell extracts of cultures grown in Translucent media supplemented with 0.1 M KCl and 0.75 mg/mL Met using anti-HA and anti-LexA antibodies (Covance and Abcam, respectively), the corresponding antimouse or antirabbit HRP secondary antibodies, and an ECL detection system (GE Healthcare). Several independent clones were used for the quantification of KAT1 protein expression in the absence and presence of BAG4. The ImageJ software (https://imagej.nih.gov/ij/) was used to quantify the bands corresponding to the LexA signal and the loading control to calculate normalized KAT1 expression.

Potassium Consumption Uptake and External Acidification in Yeast

The indicated plasmids were transformed in the PLY240 background and grown as described above in the functional complementation assay to midlog phase OD600 = 0.5–0.6 in Translucent media supplemented with auxotrophic requirements and 0.75 mg/mL Met. Cells were collected by centrifugation, washed, resuspended in sterile water, and incubated for 30 min at room temperature. External K^+ was monitored using external K^+-selective mini-electrodes. Single-barrelled borosilicate glass capillaries, 7 cm long with an external diameter of 1.5 mm, were pulled in a patch-clamp puller to get an open tip. Then, capillaries were sylanized and back-filled with K^+ ionophore I sensor (cocktail B, cat. no. 60398; Fluka) dissolved in a mixture of polyvinyl-chloride/tetrahydrofuran (40 mg/mL) at a 30:70 (v/v) ratio, as previously described (Planes et al., 2015). For the assays, ~20 mg of cells (wet weight) were resuspended in 3 mL of 10 mM MES pH 4.0 and loaded in a temperature-controlled (20°C) plexiglass cylinder chamber under continuous stirring. K^+-selective and reference electrode tips were placed in the assay medium and connected to a high-impedance differential amplifier (FD223; World Precision Instruments). In addition, a single glass pH electrode (model 5209, Crison) was also submerged into the assay medium in order to measure the external acidification to check the activation of the proton ATPase. After steady readings of both pH and external potassium K^+ signals were obtained, potassium chloride was added to a final concentration of 1 mM and then, after stable readings, values were again attained, 20 mM of Glc were added to activate the proton ATPase Pma1 and energize potassium uptake. Both the external pH and the potassium concentration were recorded for 45 min after Glc addition. The K^+ electrode signal was calibrated before and after experiments by adding potassium chloride to final concentrations of 0.1, 0.5, 1, and 10 mM in the assay media. Calibration curves render slopes around 45 mV/pK^+ unit. Both the total uptake (after 45 min) and the initial rate of K^+ uptake (slope of the curve representing the initial uptake; 5–8 min) were determined for three independent clones of each plasmid combination indicated (Fig. 3, A and B, respectively).

Two-Electrode Voltage Clamp in *Xenopus* Oocytes

KAT1 and BAG4 coding regions were cloned into a modified pGEM-HE vector (D. Becker, University of Würzburg). cRNA were synthesized from 1 μg of linearized vector using the HiScribe T7 ARCA mRNA (with tailing) kit (New England Biolab, http://www.NEB.com). Oocytes were obtained and prepared as previously described (Véry et al., 1995) and were injected with 30 ng of KAT1 cRNA or coinjected with 30 ng of KAT1 cRNA and 22.5 ng of BAG4 cRNA using a pneumatic injector. One day after oocyte injection, currents from whole oocytes bathed in K100 medium (100 mM KCl, 2 mM $MgCl_2$, 1 mM $CaCl_2$, and 10 mM HEPES/Tris pH 6) were recorded using the two-electrode voltage-clamp technique. Data acquisition and analyses were performed as previously described (Corratgé-Faillie et al., 2017). Voltage drops resulting from the series resistance of the bath were corrected by using two external electrodes connected to a bath probe (VG-2A x100 Virtual-ground bath clamp; Axon Instruments). KAT1 currents were obtained by subtraction of mean currents recorded in water-injected oocytes from the same oocyte batch. The percentage of KAT1 current increase with BAG4 was calculated as: (Mean current in the presence of BAG4 - Mean current in its absence) / Mean current in its absence.

BiFC and Coimmunoprecipitation Assays in *N. benthamiana*

All *KAT1* and *BAG4* plasmids used for the BiFC and coimmunoprecipitation experiments and to generate overexpression lines were constructed using the GoldenBraid system (Sarrion-Perdigones et al., 2013). For BiFC assays, we used pUPD2 vectors containing the N-terminal or C-terminal YFP sequence from the GoldenBraid collection. Then, we cloned *KAT1* and *BAG4* versions, compatible with the cloning system, into the pUPD2 vector. Alpha vectors containing the indicated fusion proteins and the 35S promoter and *Agrobacterium* "Nopaline Synthase" terminator were assembled and combined to generate the omega-level plasmids that were transformed into the *Agrobacterium tumefaciens* strain C58Ci. For the indicated experiments, alpha-level plasmids were constructed from these omega plasmids to generate constructs containing three or four transcriptional units. For plant infiltration, we used 4- to 5-week-old *N. benthamiana* plants grown at 24°C under a 16 h light/8 h dark photoperiod. For colocalization experiments used to determine the subcellular localization of the complex, the *KAT1-BAG4* interacting combination was coinfiltrated with a second plasmid containing either the ER marker (calreticulin targeting sequence-ChFP-KDEL retention sequence), the Sec24-mRFP ERES marker (both kindly provided by V. Pallás, Institute for Plant Molecular and Cell Biology), or the transmembrane domain of the rat α-2,6-sialyltransferase enzyme fused to the ChFP as a Golgi marker (STtmd-ChFP; Prokhnevsky et al., 2005). An *Agrobacterium* strain (C58Ci) transformed with the plasmid encoding the P19 tomato bushy stunt virus silencing suppressor was also used in all the infiltrations (Sarrion-Perdigones et al., 2013). The images were acquired using a Zeiss fluorescence confocal microscope with the following settings: YFP was excited with an Argon laser (514 nm) and detected at 516–548 nm. ChFP, RFP, and dsRED fluorescent protein were excited using the DPSS 561-10 laser (561 nm) and detected at 580–650 nm. Chloroplast autofluorescence was detected between 675 and 760 nm. The statistical analyses for KAT1-BAG4 BiFC and the organelle markers were determined by calculating the Pearson and Mander coefficients (corresponding to the range of values obtained in four independent images; Dunn et al., 2011). For coimmunoprecipitation assays, we used a pUPD2 4x-*c-myc* sequence from the Addgene collection to create the c-myc-BAG4 fusion. We combined the *KAT1*-YFP and c-myc-*BAG4* alpha vectors to build the omega plasmid containing both fusion proteins and infiltrated *N. benthamiana* leaves. Extraction of total proteins was carried out in modified PBS buffer (140 mM NaCl, 8 mM Na_2HPO_4•$7H_2O$, 2 mM KH_2PO_4, 10 mM KCl, and proteinase inhibitor, pH 7.4). The KAT1-YFP protein was purified using the GFP-trap (GFP-Trap_MA, Chromotech) according to the manufacturer's instructions. Samples of the protein extracts, the unbound material, and the KAT1 purification were separated on SDS-PAGE gels, transferred to nitrocellulose membranes, and probed with an anti-GFP antibody (clone 7.1 and 13.1 mixture, Roche) and an anti-*c-myc* antibody (clone 9E10, Roche) to detect BAG4. Immune complexes were visualized using the corresponding antimouse or antirabbit HRP secondary antibodies and an ECL detection system (GE Healthcare).

Kinetics of Plasma Membrane Accumulation in *N. benthamiana* and Arabidopsis

For transient expression in *N. benthamiana*, leaves were infiltrated, treated, and imaged as described for BiFC and coimmunoprecipitation. However, in this case, P19 silencing suppressor was not added to the infection mixture. The ImageJ software (https://imagej.nih.gov/ij/) was used to quantify the percentage of KAT1-YFP present at the plasma membrane as follows: the free draw tool was used to trace the contour of individual cells directly adjacent to the cell boarder (inside cell fluorescence). These forms were digitally enlarged by 7 pixel units using the ImageJ tool to quantify the whole-cell fluorescence. Fluorescence levels in ellipses adjacent to the cells were also quantified and used as the background measurement. The corrected total cell fluorescence (CTCF) was calculated using the following formula: Integrated density – (area of selected cell × mean fluorescence of background readings). The percentage of fluorescence signal at the plasma membrane was then calculated using the formula: $\%\ \text{fluorescence PM} = 100 - \left(\frac{\text{CTF inside fluorescence}}{\text{CTF whole cell fluorescence}} * 100\right)$. This procedure was carried out for 10 individual cells from each of the indicated conditions deriving from experiments done on different days. In order to quantify the amount of

KAT1 protein with and without BAG4 coexpression, an α1 level plasmid was constructed to combine the KAT1-YFP_myc-BAG4 omega construct (or the control) with the dsRED protein, which incorporates an HA epitope tag (dsRED-HA), in the same vector. In this way, the amount of dsRED can be used as an internal control monitoring the level of transient expression in each case, because all transcriptional units are in the same plasmid. Infected plants were observed on days 1, 2, and 3 postinfiltration by fluorescence confocal microscopy, and whole-cell protein extracts were generated from the infiltrated material by grinding 2-cm leaf discs in SDS-PAGE loading buffer. Samples were separated on SDS-PAGE and transferred, and KAT1, BAG4, and dsRED were detected using anti-GFP, anti-c-myc, and anti-HA antibodies.

For transient expression in Arabidopsis, the Col-0 control and the *bag4* mutant lines (SALK_033845 and SAIL_144_A10) were agroinfiltrated following the AGROBEST protocol (Wu et al., 2014). The plasmid used was the alpha-level plasmid containing KAT1-VENUS$_{intron}$, which included an intron in the Venus sequence (kindly provided by Stan Gelvin, Purdue University). This was required to avoid expression of the KAT1 fusion protein in the *Agrobacterium* strain. An omega vector combining the KAT1-VENUS$_{intron}$ and myc-BAG4 transcriptional units was used for the complementation assays. Confocal images were acquired as described above using the 514 laser and an emission wavelength between 515 nm and 530 nm. The quantification of the amount of KAT1-YFP at the plasma membrane was calculated as described above for 10 individual cells from each condition indicated.

Stomatal Movement Assays

The following lines were employed: the *kat1* mutant (SALK 093506, carrying the T-DNA insertion in the first exon), the *kat2* mutant (SALK 025933), and the two *bag4* mutant lines SAIL_144_A10 (carrying the T-DNA insertion in the first exon) and SALK_033845 (carrying the T-DNA insertion in the second exon; obtained from the Salk Institute Genomic Analysis Laboratory and Sessions et al. [2002]), two independent transformants that are homozygous for the *BAG4* insertion in the Col-0 and *kat1* mutant (SALK 093506, carrying the T-DNA insertion in the first exon) lines generated by the floral dipping method using an omega-level plasmid containing the c-myc-BAG4 fusion and the BASTA resistance gene. The double *kat1 kat2* mutant was generated by crossing the single mutants listed above. Plants were grown for 4–6 weeks under an 8 h light/16 h dark photoperiod at 22°C. Five leaves (each taken from different plants) from each genotype and condition were analyzed. For the dark conditions, leaves were harvested 1 h before the lights switched on and the leaf was split into two halves: one was maintained in the dark in MES solution, while the other was incubated in stomatal opening buffer (10 mM KCl, 7.5 mM iminodiacetic acid, and 10 mM MES/Tris, pH 6.2) for 2.5 h. For light treatment, the leaf was split into two halves and both were kept in 10 mM MES (pH 5.6). One half was kept in the dark and the other half was exposed to light and observed 2.5 h later. To take stomatal images, the tissue was mounted on a microscope slide and immersed in the respective solution. The stomatal aperture was defined as the ratio between the length of the stomatal aperture from the point of junction of the inner lips and the maximal width between the inner cuticular lips. For each condition, between 60 and 100 stomata were analyzed in five different plants. The entire assay was repeated three times.

Leaf Temperature Measurements

The same lines used in the stomatal movement assays were grown under an 8 h light/16 h dark photoperiod at 22°C. The thermographic camera Bosch GTC 400 C was used to generate the infrared images of the plants 1.5 h after the lights turned on. The plants were sown in individual pots such that the rosette leaves were not touching the walls of the pot, the tray, or other plants. For imaging, each plant was moved to a tray partially filled with water, to create a uniform environmental temperature around the pot. Leaf temperature was calculated using the GTC Transfer software. A total of six plants were measured for each genotype. Ten points were measured for each plant (60 data points/genotype). Data from each genotype were pooled together and statistically analyzed (Student's *t*-test) using the Graph Prism6 software.

Accession Numbers

Sequence data from this article can be found in the GenBank data libraries under accession numbers At5g46240 (*AtKAT1*); At4g18290 (*AtKAT2*); and At3g51780 (*AtBAG4*). Mutants used in this article can be obtained from the Arabidopsis Biological Resource Center under the accession numbers SALK 093506 (*kat1* mutant), SALK 025933 (*kat2* mutant), and SAIL_144_A10 and SALK_033845 (*bag4* mutant lines).

Supplemental Data

The following supplemental materials are available.

Supplemental Figure S1. BAG4 coexpression favors early activity of KAT1 in *Xenopus* oocytes.

Supplemental Figure S2. Immunodetection of myc-BAG4 protein in homozygous transgenic lines.

ACKNOWLEDGMENTS

The authors would like to thank Elena Moreno, María José Falaguer, Alejandro Mossi, Sara Aljama, José Antonio Navarro, Vicente Pallás, Daniel Franco-Aragón, Jorge Lozano, and Stan Gelvin for assistance in the completion of this work and for providing reagents.

Received February 25, 2019; accepted August 5, 2019; published August 26, 2019.

LITERATURE CITED

Anderson JA, Huprikar SS, Kochian LV, Lucas WJ, Gaber RF (1992) Functional expression of a probable *Arabidopsis thaliana* potassium channel in *Saccharomyces cerevisiae*. Proc Natl Acad Sci USA **89:** 3736–3740

Bertl A, Ramos J, Ludwig J, Lichtenberg-Fraté H, Reid J, Bihler H, Calero F, Martínez P, Ljungdahl PO (2003) Characterization of potassium transport in wild-type and isogenic yeast strains carrying all combinations of *trk1*, *trk2* and *tok1* null mutations. Mol Microbiol **47:** 767–780

Corratgé-Faillie C, Ronzier E, Sanchez F, Prado K, Kim JH, Lanciano S, Leonhardt N, Lacombe B, Xiong TC (2017) The Arabidopsis guard cell outward potassium channel GORK is regulated by CPK33. FEBS Lett **591:** 1982–1992

Doukhanina EV, Chen S, van der Zalm E, Godzik A, Reed J, Dickman MB (2006) Identification and functional characterization of the BAG protein family in *Arabidopsis thaliana*. J Biol Chem **281:** 18793–18801

Dreyer I, Antunes S, Hoshi T, Müller-Röber B, Palme K, Pongs O, Reintanz B, Hedrich R (1997) Plant K^+ channel α-subunits assemble indiscriminately. Biophys J **72:** 2143–2150

Duby G, Hosy E, Fizames C, Alcon C, Costa A, Sentenac H, Thibaud JB (2008) AtKC1, a conditionally targeted Shaker-type subunit, regulates the activity of plant K^+ channels. Plant J **53:** 115–123

Dunn KW, Kamocka MM, McDonald JH (2011) A practical guide to evaluating colocalization in biological microscopy. Am J Physiol Cell Physiol **300:** C723–C742

Eisenach C, Chen ZH, Grefen C, Blatt MR (2012) The trafficking protein SYP121 of Arabidopsis connects programmed stomatal closure and K^+ channel activity with vegetative growth. Plant J **69:** 241–251

Gierth M, Mäser P (2007) Potassium transporters in plants—Involvement in K^+ acquisition, redistribution and homeostasis. FEBS Lett **581:** 2348–2356

Hantouche C, Williamson B, Valinsky WC, Solomon J, Shrier A, Young JC (2017) Bag1 co-chaperone promotes TRC8 E3 ligase-dependent degradation of misfolded human ether a go-go-related gene (hERG) potassium channels. J Biol Chem **292:** 2287–2300

Hoang TM, Moghaddam L, Williams B, Khanna H, Dale J, Mundree SG (2015) Development of salinity tolerance in rice by constitutive-overexpression of genes involved in the regulation of programmed cell death. Front Plant Sci **6:** 175

Hurst AC, Meckel T, Tayefeh S, Thiel G, Homann U (2004) Trafficking of the plant potassium inward rectifier KAT1 in guard cell protoplasts of *Vicia faba*. Plant J **37:** 391–397

Ivashikina N, Becker D, Ache P, Meyerhoff O, Felle HH, Hedrich R (2001) K^+ channel profile and electrical properties of *Arabidopsis* root hairs. FEBS Lett **508:** 463–469

Jeanguenin L, Alcon C, Duby G, Boeglin M, Chérel I, Gaillard I, Zimmermann S, Sentenac H, Véry AA (2011) AtKC1 is a general

modulator of Arabidopsis inward Shaker channel activity. Plant J **67:** 570–582

Jiang Y, Lee A, Chen J, Ruta V, Cadene M, Chait BT, MacKinnon R (2003) X-ray structure of a voltage-dependent K^+ channel. Nature **423:** 33–41

Jones HG (1999) Use of thermography for quantitative studies of spatial and temporal variation of stomatal conductance over leaf surfaces. Plant Cell Environ **22:** 1043–1055

Kabbage M, Dickman MB (2008) The BAG proteins: A ubiquitous family of chaperone regulators. Cell Mol Life Sci **65:** 1390–1402

Kabbage M, Kessens R, Dickman MB (2016) A plant Bcl-2-associated athanogene is proteolytically activated to confer fungal resistance. Microb Cell **3:** 224–226

Knapp RT, Wong MJH, Kollmannsberger LK, Gassen NC, Kretzschmar A, Zschocke J, Hafner K, Young JC, Rein T (2014) Hsp70 cochaperones HspBP1 and BAG-1M differentially regulate steroid hormone receptor function. PLoS One **9:** e85415

Langhans M, Meckel T, Kress A, Lerich A, Robinson DG (2012) ERES (ER exit sites) and the "secretory unit concept". J Microsc **247:** 48–59

Lawson T, Blatt MR (2014) Stomatal size, speed, and responsiveness impact on photosynthesis and water use efficiency. Plant Physiol **164:** 1556–1570

Lebaudy A, Pascaud F, Véry AA, Alcon C, Dreyer I, Thibaud JB, Lacombe B (2010) Preferential KAT1-KAT2 heteromerization determines inward K^+ current properties in *Arabidopsis* guard cells. J Biol Chem **285:** 6265–6274

Lebaudy A, Vavasseur A, Hosy E, Dreyer I, Leonhardt N, Thibaud JB, Véry AA, Simonneau T, Sentenac H (2008) Plant adaptation to fluctuating environment and biomass production are strongly dependent on guard cell potassium channels. Proc Natl Acad Sci USA **105:** 5271–5276

Lee DW, Kim SJ, Oh YJ, Choi B, Lee J, Hwang I (2016) Arabidopsis BAG1 functions as a cofactor in Hsc70-mediated proteasomal degradation of unimported plastid proteins. Mol Plant **9:** 1428–1431

Lefoulon C, Waghmare S, Karnik R, Blatt MR (2018) Gating control and K^+ uptake by the KAT1 K^+ channel leveraged through membrane anchoring of the trafficking protein SYP121. Plant Cell Environ **41:** 2668–2677

Li K, Jiang Q, Bai X, Yang YF, Ruan MY, Cai SQ (2017) Tetrameric assembly of K^+ channels requires ER-located chaperone proteins. Mol Cell **65:** 52–65

Long SB, Campbell EB, Mackinnon R (2005) Crystal structure of a mammalian voltage-dependent *Shaker* family K^+ channel. Science **309:** 897–903

Mäser P, Thomine S, Schroeder JI, Ward JM, Hirschi K, Sze H, Talke IN, Amtmann A, Maathuis FJ, Sanders D, et al. (2001) Phylogenetic relationships within cation transporter families of Arabidopsis. Plant Physiol **126:** 1646–1667

Matheson LA, Hanton SL, Brandizzi F (2006) Traffic between the plant endoplasmic reticulum and Golgi apparatus: To the Golgi and beyond. Curr Opin Plant Biol **9:** 601–609

Meckel T, Hurst AC, Thiel G, Homann U (2004) Endocytosis against high turgor: Intact guard cells of *Vicia faba* constitutively endocytose fluorescently labelled plasma membrane and GFP-tagged K-channel KAT1. Plant J **39:** 182–193

Merlot S, Mustilli AC, Genty B, North H, Lefebvre V, Sotta B, Vavasseur A, Giraudat J (2002) Use of infrared thermal imaging to isolate Arabidopsis mutants defective in stomatal regulation. Plant J **30:** 601–609

Mumberg D, Müller R, Funk M (1994) Regulatable promoters of Saccharomyces cerevisiae: Comparison of transcriptional activity and their use for heterologous expression. Nucleic Acids Res **22:** 5767–5768

Nakamura RL, McKendree WL Jr., Hirsch RE, Sedbrook JC, Gaber RF, Sussman MR (1995) Expression of an Arabidopsis potassium channel gene in guard cells. Plant Physiol **109:** 371–374

Navarrete C, Petrezsélyová S, Barreto L, Martínez JL, Zahrádka J, Ariño J, Sychrová H, Ramos J (2010) Lack of main K^+ uptake systems in *Saccharomyces cerevisiae* cells affects yeast performance in both potassium-sufficient and potassium-limiting conditions. FEMS Yeast Res **10:** 508–517

Obrdlik P, El-Bakkoury M, Hamacher T, Cappellaro C, Vilarino C, Fleischer C, Ellerbrok H, Kamuzinzi R, Ledent V, Blaudez D, et al. (2004) K^+ channel interactions detected by a genetic system optimized for systematic studies of membrane protein interactions. Proc Natl Acad Sci USA **101:** 12242–12247

Pardo JM, Quintero FJ (2002) Plants and sodium ions: Keeping company with the enemy. Genome Biol **3:** S1017

Paumi CM, Menendez J, Arnoldo A, Engels K, Iyer KR, Thaminy S, Georgiev O, Barral Y, Michaelis S, Stagljar I (2007) Mapping protein-protein interactions for the yeast ABC transporter Ycf1p by integrated split-ubiquitin membrane yeast two-hybrid analysis. Mol Cell **26:** 15–25

Pilot G, Pratelli R, Gaymard F, Meyer Y, Sentenac H (2003) Five-group distribution of the Shaker-like K^+ channel family in higher plants. J Mol Evol **56:** 418–434

Planes MD, Niñoles R, Rubio L, Bissoli G, Bueso E, García-Sánchez MJ, Alejandro S, Gonzalez-Guzmán M, Hedrich R, Rodriguez PL, et al (2015) A mechanism of growth inhibition by abscisic acid in germinating seeds of *Arabidopsis thaliana* based on inhibition of plasma membrane H^+-ATPase and decreased cytosolic pH, K^+, and anions. J Exp Bot **66:** 813–825

Prokhnevsky AI, Peremyslov VV, Dolja VV (2005) Actin cytoskeleton is involved in targeting of a viral Hsp70 homolog to the cell periphery. J Virol **79:** 14421–14428

Rodríguez-Navarro A (2000) Potassium transport in fungi and plants. Biochim Biophys Acta **1469:** 1–30

Ronzier E, Corratgé-Faillie C, Sanchez F, Prado K, Brière C, Leonhardt N, Thibaud JB, Xiong TC (2014) CPK13, a noncanonical Ca^{2+}-dependent protein kinase, specifically inhibits KAT2 and KAT1 Shaker K^+ channels and reduces stomatal opening. Plant Physiol **166:** 314–326

Saponaro A, Porro A, Chaves-Sanjuan A, Nardini M, Rauh O, Thiel G, Moroni A (2017) Fusicoccin activates KAT1 channels by stabilizing their interaction with 14-3-3 proteins. Plant Cell **29:** 2570–2580

Sarrion-Perdigones A, Vazquez-Vilar M, Palací J, Castelijns B, Forment J, Ziarsolo P, Blanca J, Granell A, Orzaez D (2013) GoldenBraid 2.0: A comprehensive DNA assembly framework for plant synthetic biology. Plant Physiol **162:** 1618–1631

Sato A, Sato Y, Fukao Y, Fujiwara M, Umezawa T, Shinozaki K, Hibi T, Taniguchi M, Miyake H, Goto DB, Uozumi N (2009) Threonine at position 306 of the KAT1 potassium channel is essential for channel activity and is a target site for ABA-activated SnRK2/OST1/SnRK2.6 protein kinase. Biochem J **424:** 439–448

Schachtman DP, Schroeder JI, Lucas WJ, Anderson JA, Gaber RF (1992) Expression of an inward-rectifying potassium channel by the Arabidopsis KAT1 cDNA. Science **258:** 1654–1658

Sessions A, Burke E, Presting G, Aux G, McElver J, Patton D, Dietrich B, Ho P, Bacwaden J, Ko C, et al. (2002) A high-throughput Arabidopsis reverse genetics system. Plant Cell **14:** 2985–2994

Sieben C, Mikosch M, Brandizzi F, Homann U (2008) Interaction of the K^+-channel KAT1 with the coat protein complex II coat component Sec24 depends on a di-acidic endoplasmic reticulum export motif. Plant J **56:** 997–1006

Sottocornola B, Gazzarrini S, Olivari C, Romani G, Valbuzzi P, Thiel G, Moroni A (2008) 14-3-3 proteins regulate the potassium channel KAT1 by dual modes. Plant Biol (Stuttg) **10:** 231–236

Sottocornola B, Visconti S, Orsi S, Gazzarrini S, Giacometti S, Olivari C, Camoni L, Aducci P, Marra M, Abenavoli A, et al (2006) The potassium channel KAT1 is activated by plant and animal 14-3-3 proteins. J Biol Chem **281:** 35735–35741

Sutter JU, Campanoni P, Tyrrell M, Blatt MR (2006) Selective mobility and sensitivity to SNAREs is exhibited by the *Arabidopsis* KAT1 K^+ channel at the plasma membrane. Plant Cell **18:** 935–954

Sutter JU, Sieben C, Hartel A, Eisenach C, Thiel G, Blatt MR (2007) Abscisic acid triggers the endocytosis of the arabidopsis KAT1 K^+ channel and its recycling to the plasma membrane. Curr Biol **17:** 1396–1402

Szyroki A, Ivashikina N, Dietrich P, Roelfsema MR, Ache P, Reintanz B, Deeken R, Godde M, Felle H, Steinmeyer R, et al (2001) KAT1 is not essential for stomatal opening. Proc Natl Acad Sci USA **98:** 2917–2921

Takayama S, Reed JC (2001) Molecular chaperone targeting and regulation by BAG family proteins. Nat Cell Biol **3:** E237–E241 10.1038/ncb1001-e237

Véry AA, Gaymard F, Bosseux C, Sentenac H, Thibaud JB (1995) Expression of a cloned plant K^+ channel in *Xenopus* oocytes: Analysis of macroscopic currents. Plant J **7:** 321–332

Véry AA, Sentenac H (2003) Molecular mechanisms and regulation of K^+ transport in higher plants. Annu Rev Plant Biol **54:** 575–603

Wang Y, Hills A, Blatt MR (2014) Systems analysis of guard cell membrane transport for enhanced stomatal dynamics and water use efficiency. Plant Physiol **164:** 1593–1599

Wang Y, Holroyd G, Hetherington AM, Ng CKY (2004) Seeing "cool" and "hot"—infrared thermography as a tool for non-invasive, high-throughput screening of *Arabidopsis* guard cell signalling mutants. J Exp Bot **55:** 1187–1193

Williams B, Kabbage M, Britt R, Dickman MB (2010) AtBAG7, an Arabidopsis Bcl-2-associated athanogene, resides in the endoplasmic reticulum and is involved in the unfolded protein response. Proc Natl Acad Sci USA **107:** 6088–6093

Winter D, Vinegar B, Nahal H, Ammar R, Wilson GV, Provart NJ (2007) An "Electronic Fluorescent Pictograph" browser for exploring and analyzing large-scale biological data sets. PLoS One **2:** e718

Wu HY, Liu KH, Wang YC, Wu JF, Chiu WL, Chen CY, Wu SH, Sheen J, Lai EM (2014) AGROBEST: An efficient *Agrobacterium*-mediated transient expression method for versatile gene function analyses in *Arabidopsis* seedlings. Plant Methods **10:** 19

Xicluna J, Lacombe B, Dreyer I, Alcon C, Jeanguenin L, Sentenac H, Thibaud JB, Chérel I (2007) Increased functional diversity of plant K^+ channels by preferential heteromerization of the Shaker-like subunits AKT2 and KAT2. J Biol Chem **282:** 486–494

Yan A, Wu E, Lennarz WJ (2005) Studies of yeast oligosaccharyl transferase subunits using the split-ubiquitin system: Topological features and in vivo interactions. Proc Natl Acad Sci USA **102:** 7121–7126

Yang Y, Costa A, Leonhardt N, Siegel RS, Schroeder JI (2008) Isolation of a strong *Arabidopsis* guard cell promoter and its potential as a research tool. Plant Methods **4:** 6

Young JC (2014) The role of the cytosolic HSP70 chaperone system in diseases caused by misfolding and aberrant trafficking of ion channels. Dis Model Mech **7:** 319–329

Zhang B, Karnik R, Waghmare S, Donald N, Blatt MR (2017) VAMP721 conformations unmask an extended motif for K^+ channel binding and gating control. Plant Physiol **173:** 536–551

Zhang B, Karnik R, Wang Y, Wallmeroth N, Blatt MR, Grefen C (2015) The Arabidopsis R-SNARE VAMP721 interacts with KAT1 and KC1 K^+ channels to moderate K^+ current at the plasma membrane. Plant Cell **27:** 1697–1717